Three-Meson Resonances in a Relativistic Faddeev-Type Approach*

G. Mennessier and J.-Y. Pasquier
Laboratoire de Physique Théorique et Hautes Energies, 91-Orsay, France†

and

R. Pasquier
Institut de Physique Nucléaire, Division de Physique Théorique, 91-Orsay, France†
(Received 3 April 1969; revised manuscript received 16 May 1972)‡

Three-body resonances are studied within the framework of a relativistic version of the Faddeev equations, in which the input two-body amplitudes are assumed to be separable. A first discussion concerns the simplest $\pi\pi\pi$ and $K\bar{K}\pi$ systems in which only the ρ(765 MeV) or the K^*(890 MeV) resonance is taken into account. Compared to preceding works on a similar subject, more flexible parametrizations are used, allowing us to consider a larger class of two-body interactions and to better understand the influence of the main parameters involved in the model. A more satisfactory agreement with experiment is also found in the three-pion case and this for more realistic two-body amplitudes. The success is less convincing for the $K\bar{K}\pi$ case, but this might be due to the neglect of the two-body $K\bar{K}$ interaction. Finally the study of the $K\pi\pi$ case gives an insight into the constructive and destructive interference effects which can be observed when more than one two-body resonance is taken into account. We add in the Appendix some comments about the properties one can reasonably require for the input separable two-body amplitudes owing to potential theory or its relativistic generalizations.

I. INTRODUCTION

In the nonrelativistic case, the Faddeev equations[1] provide a useful tool for investigating three-particle problems. Several groups have tried to make relativistic generalizations with possible applications to higher-energy processes. They usually start from the three-particle analogs of the Bethe-Salpeter equation[2] which may be written in the Faddeev form after some transformations.[3] When the particles are assumed to interact through two-body forces only, this yields

$$T_i = t_i + \sum_{j \neq i} t_i G_i^0 T_j , \tag{1.1}$$

where $T = \sum_i T_i$ stands for the three-body T matrix, t_i describes the scattering of the particles j and k, and G_i^0 is the free Green's function.

A peculiar difficulty of Eq. (1.1) compared to the nonrelativistic case comes from the presence of extra variables of integration – the fourth components of the off-shell intermediate particles momenta – which must be eliminated if the equations are to be tractable numerically. A method for doing so was first given by Blankenbecler and Sugar[4] for two-particle scattering. Different procedures have been proposed for the three-body case.[4-7] They lead to equations still having the form of (1.1) but with only the total energy as an off-shell variable and a modified propagator, E_i^0 say, in place of G_i^0. A further simplification occurs when the input two-body amplitudes can be approximated by separable forms as might be expected when these amplitudes are dominated by bound states or resonances.[8] The T_i matrix elements between states of given angular momenta then satisfy one-dimensional integral equations which may be amenable to practical computations.

In the present work, we restrict ourselves to three-meson systems AAB or $A\bar{A}B$ in which two particles at least are identical or charge conjugates. Previous numerical results have already been obtained in the $\pi\pi\pi$ case.[9-11] However, additional investigations, both theoretical and numerical, would be useful to understand their deep significance and reliability. One purpose of this paper is to contribute to this task by looking at the three-body resonances in the three simple $\pi\pi\pi$, $K\bar{K}\pi$, and $K\pi\pi$ (or $\bar{K}\pi\pi$) systems.

Section II is devoted to a general treatment of the basic integral equations. After the partial-wave decomposition, these are written in a one-dimensional form by assuming the two-body amplitudes to be separable with respect to the initial and final off-shell momenta.

In Sec. III we examine a rather simplified approach to the $\pi\pi\pi$ and $K\bar{K}\pi$ cases where either the ρ or the $K^*(\bar{K}^*)$ resonance is taken into account (Sec. III A). All the parametrizations given in Sec. III B for the input two-body amplitudes are chosen in order to ensure two-body unitarity (and thus three-body unitarity)[5-7] and to represent reason-

ably well the phase shift in the neighborhood of the two-body resonance. Other constraints are deduced by extrapolating results obtained within the framework of potential theory. These are reviewed in a shortened way in the Appendix, on the basis of a preceding work by one of us.[12] Once the two-body amplitude is chosen, the three-body integral equations are solved by techniques which are explained in Sec. III C. On the other hand, Secs. III D and III F are devoted to a discussion about the influence of the parameters involved in the model on the three-body results. The latter are compared with experiment in Sec. III E.[13]

Section IV is devoted to the more complicated $K\pi\pi$ case,[14] in which both the ρ and K^* resonances are assumed to contribute. This gives an insight into the constructive and destructive interference effects which can be observed where more than one two-body resonance is taken into account in the problem.

A general discussion about the reliability of the results obtained in the present work and a short comparison with those observed in a dispersive model for the three-pion case are inserted in the Conclusion.

II. BASIC INTEGRAL EQUATIONS

In explicit form, our starting equations read

$$\begin{aligned}&\langle \vec{q}_1\vec{q}_2\vec{q}_3\tau_{1z}\tau_{2z}\tau_{3z}\,|\,T_i(s)\,|\rangle\\ &\quad=\langle \vec{q}_1\vec{q}_2\vec{q}_3\tau_{1z}\tau_{2z}\tau_{3z}|\,t_i(\sigma_i)\,|\,\rangle\\ &\quad+\sum_{j\neq i}\sum_{\tau'_{1z}\tau'_{2z}\tau'_{3z}}\int\langle \vec{q}_1\vec{q}_2\vec{q}_3\tau_{1z}\tau_{2z}\tau_{3z}|\,t_i(\sigma_i)\,|\vec{q}'_1\vec{q}'_2\vec{q}'_3\tau'_{1z}\tau'_{2z}\tau'_{3z}\rangle\\ &\qquad\times E_i^0(s,\omega'_1,\omega'_2,\omega'_3)\langle \vec{q}'_1\vec{q}'_2\vec{q}'_3\tau'_{1z}\tau'_{2z}\tau'_{3z}|\,T_j(s)\,|\rangle\,\delta^3\Big(\sum_i \vec{q}'_i-\sum_i \vec{q}_i\Big)\frac{d^3q'_1}{2\omega'_1}\frac{d^3q'_2}{2\omega'_2}\frac{d^3q'_3}{2\omega'_3}\,,\end{aligned}\tag{2.1}$$

where the three-meson states $\langle \vec{q}_1\vec{q}_2\vec{q}_3\tau_{1z}\tau_{2z}\tau_{3z}|$ are labeled by the momenta $\vec{q}_i$ and the third isospin components τ_{iz} of each particle (we omit the initial state which plays no essential role in the present investigations). These states are normalized according to

$$\langle \vec{q}_1\vec{q}_2\vec{q}_3\tau_{1z}\tau_{2z}\tau_{3z}|\,\vec{q}'_1\vec{q}'_2\vec{q}'_3\tau'_{1z}\tau'_{2z}\tau'_{3z}\rangle=\prod_{i=1,2,3}2\omega_i\delta^3(\vec{q}_i-\vec{q}'_i)\delta_{\tau_{iz}\tau'_{iz}}\,.\tag{2.2}$$

Correspondingly, we have

$$\langle \vec{q}_1\vec{q}_2\vec{q}_3\tau_{1z}\tau_{2z}\tau_{3z}|\,t_i(\sigma_i)\,|\vec{q}'_1\vec{q}'_2\vec{q}'_3\tau'_{1z}\tau'_{2z}\tau'_{3z}\rangle=2\omega_i\delta^3(\vec{q}_i-\vec{q}'_i)\delta_{\tau_{iz}\tau'_{iz}}\langle \vec{q}_j\vec{q}_k\tau_{jz}\tau_{kz}|\,\hat{t}_i(\sigma_i)\,|\vec{q}'_j\vec{q}'_k\tau'_{jz}\tau'_{kz}\rangle\,,\tag{2.3}$$

where $\langle\,|\hat{t}_i(\sigma_i)|\,\rangle$ is the usual two-body amplitude. $\omega_i=(q_i^{\,2}+m_i^{\,2})^{1/2}$ is the energy of the particle i and σ_i is the squared invariant energy of the (j,k) subsystem. In the three-body c.m. system, these two variables are related to the three-body invariant s through

$$\sigma_i=s+m_i^{\,2}-2\omega_i\sqrt{s}\,.\tag{2.4}$$

We choose for the propagator E_i^0 the expression

$$E_i^0(s,\omega_1,\omega_2,\omega_3)=\frac{2}{\pi}\sum_{i=1,2,3}\omega_i\Big/\Big[\Big(\sum_{i=1,2,3}\omega_i\Big)^2-s\Big]\,,\tag{2.5}$$

which indeed does not depend upon the index i. With these conventions, the three-body unitarity relations for $T=\sum_{i=1,2,3}T_i$ read

$$T-T^\dagger=2iTT^\dagger=2iT^\dagger T\tag{2.6}$$

provided that

$$\hat{t}_i-\hat{t}_i^\dagger=2i\hat{t}_i\hat{t}_i^\dagger=2i\hat{t}_i^\dagger\hat{t}_i\tag{2.6'}$$

for any $\hat{t}_i$.

Now, from Eq. (2.1) we can derive equations for the matrix elements of the T_i between states of definite total angular momentum and isospin. To define such states, we let one of the three particles play a privileged role, e.g., particle i. In the three-body c.m. system, convenient labels are the following:

(1) The three lengths q_1, q_2, q_3 of the momenta $\vec{q}_i$, which we denote more concisely as $\{q\}$.

(2) J, the length of the total angular momentum; M, its projection along the z axis of a space-fixed frame; Λ_i, its projection along the z axis of a body-fixed frame. To define the latter, we use the helicity convention,[15,16] i.e., the z axis is chosen in the direction of $-\vec{q}_i = \vec{q}_j + \vec{q}_k$. The corresponding y axis lies in the direction of $\vec{q}_i \times \vec{q}_j$ with (i, j, k) cyclic. Λ_i is then nothing but the helicity of the (j, k) subsystem.

(3) The parity P. The appropriate eigenstates of parity P are[16]

$$|JM\Lambda_i P\rangle = \tfrac{1}{2}[\,|JM\Lambda_i\rangle + \eta(-)^{J+\Lambda_i}|JM-\Lambda_i\rangle\,], \tag{2.7}$$

where η is the product of P and of the intrinsic parities of the three particles.

(4) I_i, the isospin of the pair (j, k), and $\mathcal{I}$ and $\mathcal{I}_z$, the total isospin and its third component.

Passing from the basis $\langle \vec{q}_1\vec{q}_2\vec{q}_3\tau_{1z}\tau_{2z}\tau_{3z}|$ of the Hilbert space to the basis $\langle \{q\}JM\Lambda_i PI_i\,\mathcal{I}\mathcal{I}_z|$ is completely determined by Eq. (2.7) and the relation

$$\langle \vec{q}_1\vec{q}_2\vec{q}_3\tau_{1z}\tau_{2z}\tau_{3z}| = \sum_{JM\Lambda_i I_i \mathcal{I}\mathcal{I}_z} (2J+1)^{1/2}\mathfrak{D}^{J*}_{M\Lambda_i}(\mathcal{E}_i)\langle \tau_i\tau_{iz}I_iI_{iz}|\,\mathcal{I}\mathcal{I}_z\rangle\langle \tau_j\tau_{jz}\tau_k\tau_{kz}|I_iI_{iz}\rangle\langle \{q\}JM\Lambda_i I_i\,\mathcal{I}\mathcal{I}_z| \tag{2.8}$$

with (i, j, k) cyclic. $\mathcal{E}_i$ stands for the three Euler angles of the rotation which transforms the space-fixed frame into the helicity frame having $-\vec{q}_i$ as the z axis. Correspondingly, if we introduce the usual two-body amplitude $\hat{t}^{I_i}_{il_i}$ of definite two-body angular momentum l_i and isospin I_i, we can expand (2.3) as

$$\begin{aligned}&\langle \vec{q}_1\vec{q}_2\vec{q}_3\tau_{1z}\tau_{2z}\tau_{3z}|\,t_i(\sigma_i)\,|\vec{q}_1'\vec{q}_2'\vec{q}_3'\tau_{1z}'\tau_{2z}'\tau_{3z}'\rangle\\ &\quad= \sum_{J\Lambda_i\Lambda_i' l_i I_i \mathcal{I}\mathcal{I}_z} (2J+1)\mathfrak{D}^{J*}_{\Lambda_i'\Lambda_i}(\mathcal{E}_i'^{-1}\mathcal{E}_i)\frac{2}{q_i}\delta(\omega_i-\omega_i')\delta_{\Lambda_i\Lambda_i'}\delta_{\tau_{iz}\tau_{iz}'}\langle \tau_i\tau_{iz}I_iI_{iz}|\,\mathcal{I}\mathcal{I}_z\rangle\langle \tau_j\tau_{jz}\tau_k\tau_{kz}|I_iI_{iz}\rangle\\ &\qquad\times Y^{\Lambda_i}_{l_i}(\theta_i,0)\hat{t}^{I_i}_{il_i}(p_i,\sigma_i,p_i')Y^{\Lambda_i}_{l_i}(\theta_i',0)\langle I_iI_{iz}|\,\tau_j\tau_{jz}'\tau_k\tau_{kz}'\rangle\langle \mathcal{I}\mathcal{I}_z|\,\tau_i\tau_{iz}'I_iI_{iz}\rangle\end{aligned} \tag{2.9}$$

with (i, j, k) cyclic. p_i (p_i') is the common value of the lengths of the (j) and (k) initial (final) momenta in the (j, k) c.m. system. θ_i (θ_i') is the angle between the momenta of the particles (i) and (j) in the same c.m. system.

The preceding relations allow one to write two-dimensional integral equations for the matrix elements $\langle \{q\}JM\Lambda_i PI_i\,\mathcal{I}\mathcal{I}_z|\,T_i|\rangle$. These equations reduce to one dimension when the input two-body off-shell amplitudes $\hat{t}^{I_i}_{il_i}(p_i,\sigma_i,p_i')$ are assumed separable in p_i and p_i'.

In fact, we restrict ourselves in this work to the use of separable forms of the type

$$\hat{t}^{I_i}_{il_i}(p_i,\sigma_i,p_i') = \frac{g^{I_i}_{il_i}(p_i)g^{I_i}_{il_i}(p_i')}{D^{I_i}_{il_i}(\sigma_i)} \tag{2.10}$$

because of their simplicity and for comparison with preceding works. The condition of unitarity for such representations is fulfilled by imposing

$$D^{I_i}_{il_i}(\sigma_i) = P(\sigma_i) - \frac{1}{\pi}\int_{(m_j+m_k)^2}^{\infty}\frac{d\sigma_i'}{\sigma_i'-\sigma_i}\rho_i(\sigma_i')[g^{I_i}_{il_i}(p_i(\sigma_i'))]^2\,, \tag{2.11}$$

where $P(\sigma)$ stands for an arbitrary polynomial of σ and ρ_i for the phase-space factor

$$\rho_i(\sigma) = \pi p_i(\sigma)/\sqrt{\sigma}\,, \tag{2.12}$$

with

$$p_i(\sigma) = \frac{\{[\sigma-(m_j-m_k)^2][\sigma-(m_j+m_k)^2]\}^{1/2}}{2\sqrt{\sigma}}\,. \tag{2.12'}$$

The particular form of (2.9) and (2.10) then suggests the change of function

$$\langle \{q\}JM\Lambda_i PI_i\,\mathcal{I}\mathcal{I}_z|\,T_i|\rangle = \langle \{q\}JM\Lambda_i PI_i\,\mathcal{I}\mathcal{I}_z|\,t_i|\rangle + \sum_{l_i} g^{I_i}_{il_i}(p_i)Y^{\Lambda_i}_{l_i}(\theta_i,0)B^{\Lambda_i I_i}_{il_i}(q_i)\,. \tag{2.13}$$

As one can check, the functions of a single variable $B^{\Lambda_i I_i}_{il_i}(q_i)$ possess well-defined symmetry properties in the change $\Lambda_i \to -\Lambda_i$, which follow from the corresponding properties of the parity eigenstates[16] and of the spherical harmonics. More explicitly, we have

$$B^{-\Lambda_i I_i}_{il_i}(q_i)=\eta(-)^J B^{\Lambda_i I_i}_{il_i}(q_i)\,. \tag{2.14}$$

This makes it sufficient to consider only amplitudes $B^{\Lambda_i I_i}_{il_i}(q_i)$ having $\Lambda_i \geq 0$ [indeed, from Eq. (2.14), some of them for which $\Lambda_i = 0$ vanish identically]. The reduced set of amplitudes $B^{\Lambda_i I_i}_{il_i}(q_i)$ satisfy integral equations which read finally

$$B^{\Lambda_i I_i}_{il_i}(q_i)=B^{\Lambda_i I_i}_{0l_i}(q_i)+\sum_{j\neq i}\sum_{l'_j I'_j}\sum_{\Lambda'_j\geq 0} C_{I_i I'_j}\frac{1}{D^{I_i}_{il_i}(\sigma_i)}\int_0^\infty dq'_j\, {}^{I_i\Lambda_i}_{l_i i}K^{\Lambda'_j I'_j}_{jl'_j}(q_i,q'_j)B^{\Lambda'_j I'_j}_{jl'_j}(q'_j)\,. \tag{2.15}$$

The detailed expression of the inhomogeneous term B_0 of this equation is irrelevant for the present purpose, i.e., the study of three-body resonances but not the Dalitz-plot distributions: This requires only the properties of the kernel CK/D. The general form of the kernel K is

$${}^{I\Lambda}_{l i}K^{\Lambda' I'}_{jl'}(q_i,q'_j)=\frac{q'^2_j}{\omega'_j}\int_{-1}^{+1}d\xi\,{}^{\Lambda}_{l i}F^{\Lambda'}_{jl'}(q_i,q'_j,\xi)\frac{1}{\omega'_k}\frac{2}{\pi}\frac{\omega_i+\omega'_j+\omega'_k}{(\omega_i+\omega'_j+\omega'_k)^2-s}\frac{g^I_{il}(p_i(\sigma'_{jk}))}{[p_i(\sigma'_{jk})]^l}\frac{g^{I'}_{jl'}(p_j(\sigma'_{ik}))}{[p_j(\sigma'_{ik})]^{l'}}\,, \tag{2.16}$$

with

$$\begin{aligned}&\xi=\cos\chi'_{ij}\,, \qquad q'^2_k=q_i^2+q'^2_j+2q_iq'_j\xi\,,\\ &\omega'_k=(q'^2_k+m_k^2)^{1/2}\,, \qquad \sigma'_{jk}=(\omega'_j+\omega'_k)^2-q_i^2\,;\end{aligned} \tag{2.17}$$

$$\begin{aligned}&{}^{\Lambda}_{l i}F^{\Lambda'}_{jl'}=2\pi^2\epsilon_{\Lambda'}[p_i(\sigma'_{jk})]^l[p_j(\sigma'_{ik})]^{l'}Y^{\Lambda}_l(\theta'_i,0)Y^{\Lambda'}_{l'}(\theta'_j,0)\tfrac{1}{2}[d^J_{\Lambda\Lambda'}(\chi'_{ij})+\eta(-)^{J+\Lambda'}d^J_{\Lambda-\Lambda'}(\chi'_{ij})]\,,\\ &\epsilon_{\Lambda'}=1\ (2)\ \text{ if }\ \Lambda'=0\ (\geq 1)\,.\end{aligned} \tag{2.18}$$

In the expression for F, the two d functions are nothing but recoupling coefficients between the different i and j angular momentum bases. The coefficients $C_{I_i I_j}$ in (2.15) play the same role for the isospin.

The coupled system (2.15) can be further reduced, if we take into account the fact that two particles at least are identical or charge conjugates. In the $\pi\pi\pi$ and $K\pi\pi$ cases, Bose-Einstein statistics impose the full amplitude $\langle \vec{q}_1\vec{q}_2\vec{q}_3\tau_{1z}\tau_{2z}\tau_{3z}|\,T\,|\rangle$ to be invariant in the exchange of two pions. In the $K\bar{K}\pi$ case, similar symmetry properties occur with respect to the exchange of the K and the $\bar{K}$ if the initial state is an eigenstate of G parity. Relations (2.8) and (2.13) imply correspondingly well-defined relations between the B amplitudes, which are specified below for each system separately. When these relations are inserted in Eq. (2.15), we find that different equations become equivalent, thus enabling one to consider only a restricted number of them. In fact, we can always completely remove the coupling by channel indices j, but this sometimes requires one iteration as done in Sec. IV for the $K\pi\pi$ case. Finally, when only one type of resonance is retained in each two-body system,[17] only a coupling by helicity indices Λ_i (or, equivalently, a coupling between resonance + particle states of different angular momenta) remains.

III. DISCUSSION ON THE $\pi\pi\pi$ AND $K\bar{K}\pi$ CASES

A. Reduction of the Equations

For several reasons, the $\pi\pi\pi$ system provides a convenient field for testing the reliability of the approximations introduced in the preceding section. First, there is the large amount of experimental information, especially as concerns the three-body resonances. Next, there is the simplicity, resulting largely from the identity of the three particles. Indeed in this case, Bose-Einstein statistics impose relations between the amplitudes B_i of Eq. (2.13). These read explicitly

$$B^{\Lambda I}_{1l}(q)=B^{\Lambda I}_{2l}(q)=B^{\Lambda I}_{3l}(q)\,, \tag{3.1}$$

with $l+I$ even.

Less experimental information has been collected as regards the $K\bar{K}\pi$ system. There are, nevertheless, numerous studies about the so-called D and E mesons and about Dalitz-plot distributions.[18] This time again, symmetry relations are imposed on the amplitudes B_i. They are obtained by observing that the $K\bar{K}\pi$ states of given G parity G have well-defined symmetry properties in the exchange of the K and $\bar{K}$ doublets. More explicitly, we must have

$$B^{\Lambda I}_{2l}(q)=G(-)^{I+I-1-\tau_K}B^{\Lambda I}_{1l}(q) \tag{3.2}$$

and

$$B^{\Lambda_3 I_3}_{3 I_3}(q_3)=0 \ \text{ unless } \ G=(-)^{I_3+I_3-1}\,. \tag{3.2'}$$

(The index 3 refers to the $K\bar{K}$ channel.[13])

As pointed out above, the symmetry conditions (3.1), (3.2), and (3.2′) enable one to remove the coupling through the channel indices i of Eqs. (2.15). However, these equations still remain

coupled through Λ, l, and I. A great simplification occurs when only one type of two-body resonance (i.e., one value of l and I) is kept in the problem.

Here, the two-body $\pi\pi$ and $K\pi$ amplitudes are assumed to be determined only by the $\rho(l=1,\ I=1)$ and $K^*(l=1,\ I=\frac{1}{2})$ resonances, respectively. A reasonable representation of the three-pion system can be expected in this way in the 1.0–1.5-GeV region where the three-body resonances – and in particular the so-called A mesons – decay essentially through $\pi\rho$ states. As concerns the $K\bar{K}\pi$ system, the approximation seems less reasonable since in many Dalitz-plot distributions, not only the K^* but also an $I=1$ enhancement in the $K\bar{K}$ subsystem appear important. However, the nature and the characteristics of this $K\bar{K}$ object are not yet completely established (see, for instance, Ref. 19). It would thus be difficult to include it in an actual numerical calculation.

To retain only the ρ and the K^*, which are both $l=1$ resonances, allows at the same time a similar treatment of the $\pi\pi\pi$ and $K\bar{K}\pi$ systems, as would indeed be possible within the framework of SU(3) symmetry. In both cases, by omitting many of the indices and summations which now become unnecessary, we can finally reduce the integral equations to

$$B^{\Lambda}(q) = B_0^{\Lambda}(q) + \alpha C(\mathcal{g}) \times \sum_{\Lambda'=0,\,1} \frac{1}{D(\sigma)} \int_0^{\infty} dq'\, {}_1K_2^{\Lambda\Lambda'}(q, q') B^{\Lambda'}(q') . \tag{3.3}$$

The value of α is $-2G$ ($G=-1$) in the $\pi\pi\pi$ case, G in the $K\bar{K}\pi$ case; the difference comes, among other reasons, from the neglect of the $K\bar{K}$ interaction, which implies that $B_{3l_3}^{\Lambda 3 I_3}$ identically vanishes in the $K\bar{K}\pi$ case. The isospin coefficients $C(\mathcal{g})$ are quoted in Tables I(a) and I(b). The two-body energy invariant σ associated with the particle of impulsion $q=(\omega^2-m^2)^{1/2}$ and mass $m=m_\pi$ or m_K is given as in Eq. (2.4).

B. Choice of the Two-Body Amplitude

To solve Eq. (3.3) we must first give the factors $g_l(p)$ and $D_l(\sigma)$ which enter the representation (2.10) (for simplicity, the indices I and i are omitted). In this connection, it is worthwhile to recall that the experimental information that we possess about $\pi\pi$ and $K\pi$ amplitudes only concerns on- and off-mass-shell quantities from which it is difficult to extract in a nonambiguous way[5] the off-energy-shell amplitudes. It seems therefore more convenient to represent these amplitudes by simple parametrizations allowing one to satisfy general principles such as two-body unitarity and time-reversal invariance, and to take into account the results deduced from reasonable dynamical models of potential theory or of its relativistic generalizations. As an example, we briefly recall in the Appendix the amount of information that potential theory can give. Many of the properties which are so reviewed remain also valid in relativistic treatments: They are found for instance within the equations of Blankenbecler and Sugar.[4,20,21]

TABLE I. The isospin coefficients $C(\mathcal{g})$ of Eq. (3.3) according to the value of $\mathcal{g}$, (a) in the $\pi\pi\pi$ case, (b) in the $K\bar{K}\pi$ case.

	(a)	
$\mathcal{g}$	0	1 and 2
$C(\mathcal{g})$	1	$-\frac{1}{2}$
	(b)	
$\mathcal{g}$	0	1
$C(\mathcal{g})$	-1	$-\frac{1}{3}$

Let us begin with a review of some simple parametrizations of (2.10) having two-body unitarity built in and which *a priori* can be used in the problem.

The simplest one, which at the same time allows us easily to fulfill the conditions (see Ref. 5 and the Appendix)

$$g_l(p) = O(p^l) \quad \text{as} \quad p \to 0 , \tag{3.4}$$

$$g_l(p) = O(p^{-l-2+2r}) \quad \text{as} \quad p \to \infty \tag{3.5}$$

(r is a positive or null integer depending on the potential), is obtained by writing

$$g_l^2(p) = \frac{p^{2l}}{(p^2+\mu^2)^n} , \tag{3.6}$$

with n an integer and μ^2 real (see Refs. 6 and 9). Another similar representation is

$$g_l^2(p) = p^{2l} \sum_{h=1}^{n} \frac{R_h}{p^2+\mu_h^2} , \tag{3.6'}$$

with R_h and μ_h^2 real. In both cases, the function $D_l(\sigma)$ is given by a dispersion integral like (2.11). Note also that the singularities of $g_l(p)$ as given by Eq. (3.6) and (3.6′) lie on the negative real p^2 axis. This agrees with an analogy often suggested between $g_l^2(p)$ and the N function of the usual ND^{-1} decomposition.[8]

The same analogy is also transparent through the representation[22]

$$D_l(\sigma) = \epsilon \exp\left[-\frac{\sigma-\sigma_1}{\pi} \int_{(m_j+m_k)^2}^{\infty} \frac{d\sigma' \delta_l(\sigma')}{(\sigma'-\sigma)(\sigma'-\sigma_1)} \right] . \tag{3.7}$$

[σ_1 is some subtraction point. At infinity, $D(\sigma)$

$= O(1)$ or $O(\sigma)$ depending on whether $\delta_l(\sigma)$ tends towards 0 or π.]

$$g_l^2(p(\sigma)) = D_l(\sigma)[e^{i\delta_l(\sigma)} \sin\delta_l(\sigma)]/\rho(\sigma). \qquad (3.8)$$

m_j and m_k are the masses of the particles of the two-body system which is considered; $\rho(\sigma)$ and $p(\sigma)$ are given as in Eqs. (2.12) and (2.12′). The constant ϵ in (3.7) is suitably chosen equal to ± 1 in order that g_l^2 be positive. $\delta_l(\sigma)$ can be conveniently parametrized through an effective-range formula of the type

$$\frac{p^2(\sigma)}{p_r^2}\frac{\rho(\sigma)}{\rho_r}\cot\delta_l(\sigma) = a + b\frac{p^2}{p_r^2} + c\left(\frac{p^2}{p_r^2}\right)^n, \qquad (3.9)$$

with p_r and ρ_r the values of $p(\sigma)$ and $\rho(\sigma)$ at the two-body resonance energy σ_r. The numerical integration of (3.7) gives $D_l(\sigma)$ and then $g_l^2(p)$. The result can be represented by rational fractions through least-squares-fit techniques. The final analytic form of $g_l^2(p)$ looks like Eq. (3.6′) but the poles and the residues are generally complex, as the analysis in the Appendix indeed suggests (see also Ref. 11). A similar result is obtained in a simpler way with a slightly changed effective-range development deduced by replacing $\rho(\sigma)$ in the left-hand side of Eq. (3.9) by $\rho(\sigma)/[\sigma - (m_j - m_k)^2]^{1/2}$. The main properties of $\delta_l(\sigma)$ in the two-body physical region are not greatly affected and the procedure allows an analytic integration of Eq. (3.7). The missing factor appears again in the final representation of $g_l^2(p)$, which reads

$$g_l^2(p) = [\sigma - (m_j - m_k)^2]^{-1/2} p^{2l} \sum_{h=1}^{n} \frac{r_{\rm ch}}{p^2 + \mu_{\rm ch}^2}, \qquad (3.10)$$

with $r_{\rm ch}$ and $\mu_{\rm ch}^2$ generally complex. (This factor may be considered as simulating some sort of left-hand cut.)

Now the question concerns the precise values of the parameters involved in the above representations. Besides conditions (3.4) and (3.5), we have to require first that $D_l(\sigma)$ vanish on its second sheet at a point σ_R ($\sigma_r = {\rm Re}\sigma_R$) whose position is well determined from the characteristics of the two-body resonance. As discussed in the Appendix on the basis of rather reasonable two-body interactions, other general constraints can be imposed on the analytic properties of the $g_l^2(p)$, but they still leave some freedom for determining this function completely, unless some peculiar parametrizations are used. In this connection, it seems equally natural either to assume that (2.10) reduces to the on-shell amplitude for $p^2 = p'^2 = P^2$, or to impose instead the correct off-shell behavior in the vicinity of the resonance pole. The simple form (2.10) or (A8) does not enable one to fulfill both properties simultaneously (see the Appendix). Therefore the function $g_l(p)$, which in the three-body equations best accounts for the effects of the initial two-body amplitude, can only satisfy each of these two assumptions in a more or less approximate way, according to the energy region.

Let us nevertheless assume for a time that the second is fulfilled, which by the way is enabling one to easily build up a framework for further discussions. As examined in the Appendix, the $\delta_l(\sigma)$ function is then above all a convenient intermediate quantity whose relationship with the experimental phase shift makes full sense only near $\sigma = \sigma_r$. Then only $\delta_l(\sigma)$ and its first derivative at σ_r may be reasonably expected to equal the corresponding experimental quantities, which are simply related to the position σ_r and the width Γ_r of the two-body resonance. These two quantities enable one to fix two parameters of the problem, which together with the asymptotic behavior (3.5) is sufficient to determine n and μ^2 in (3.6) and $P(\sigma)$ in (2.11), provided that the latter is a constant. Some freedom remains, however, for the other less rigid representations and the resulting $\delta_l(\sigma)$ functions, although very similar in the vicinity of σ_r, may differ largely elsewhere. This leads us to consider the three main types of $g_l^2(p(\sigma))$ and $\delta_l(\sigma)$ functions which are illustrated in Figs. 1 and 2 for the $\pi\pi$ case as an example [$\delta_l(\sigma)$ is always assumed to vanish at threshold]. The three types may be differentiated by the values of any one of the parameters in Eq. (3.9). Here we have chosen c which governs the deviations of Eq. (3.9) from the usual scattering-length formula. Two values of this parameter appear of particular importance, namely $c = c_0$ and $c = 0$ with

$$c_0 = -a_0/(n-1), \qquad (3.11)$$

where $a_0 = 4p_r^2/\Gamma_r\sqrt{\sigma_r}$ is the inverse of the scattering length obtained by fitting the mass of the two-body resonance when $c = 0$ (see Ref. 23 for the $\pi\pi$ case). Indeed just at $c = c_0$, the two-body scattering length is infinite ($a = 0$), while at $c = 0$, the three-body equations do not necessarily converge. In this context type I corresponds to $c < c_0$, type II to $c_0 < c < 0$, and type III to $c > 0$.

The consideration of these three types as well as continuous variations of the free parameter c in (3.9) will allow one to understand better the influence in the model of the parameters related to the two-body amplitude. Note that this can also enable one to compare our results with those of preceding works. Indeed, type I in Figs. 1(a) and 2(a) is just that obtained with the simplest parametrization (3.6), used in Refs. 9 and 10. On another side,

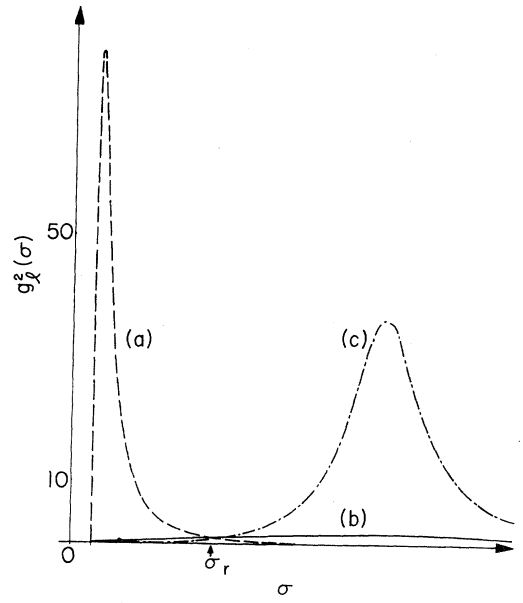

FIG. 1. The three types of $g_l^2(p(\sigma))$ factors considered in the $\pi\pi\pi$ case. Curve (a) illustrates type I and is obtained with the representation (3.6). Curves (b) and (c) illustrate types II and III. They have been obtained with the representation (3.10) with respectively $c = -0.33$ and $c = +0.33$ in the corresponding parametrization (3.9) of $\delta_l(\sigma)$.

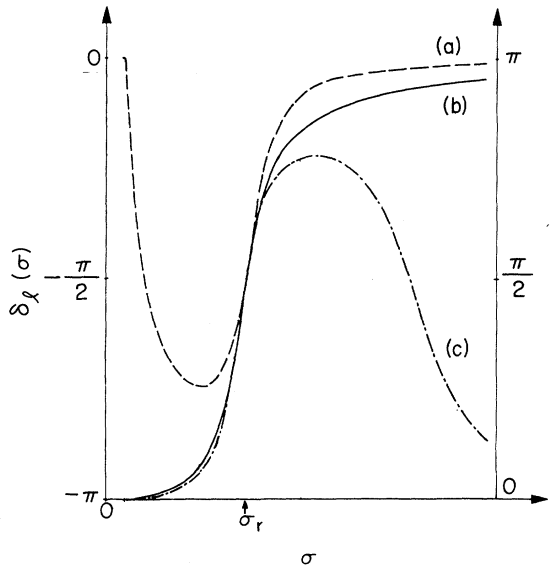

FIG. 2. The $\delta_l(\sigma)$ functions corresponding to the three g_l^2 factors of Fig. 1. The left- and the right-hand ordinate scales are associated, respectively, with curve (a) and curves (b), (c).

type II in Figs. 1(b) and 2(b) just corresponds to the choice – the on-shell one – which is mainly used in the dispersive on-shell model of Refs. 24 and 25. (Other applications of the same type of model may be found in Ref. 26.)

Owing to the discussion of the Appendix, let us now look at the ability of each type to represent the true two-body amplitude $\hat{t}_l(p,\sigma,p')$ needed in the basic three-body equations.

Type I illustrated in Figs. 1(a) and 2(a) appears in this context to exhibit several unpleasant features: The more inconvenient concerns the singularities of the $g_l^2(p)$ which lie deeply inside the analyticity parabola $\mathcal{P}(\mu^2 = 4)$ introduced in the Appendix, Eq. (A7′). (Indeed, for $c \simeq c_0$, they lie nearby the physical region and the two-body threshold.) On the other hand, as the behavior of the associated $\delta_l(\sigma)$ function (negative scattering length) suggests, this type might correspond to repulsive two-body forces,[27] which seems somewhat unreasonable for a resonant amplitude and does not agree with the experimental information.

Type II [Figs. 1(b) and 2(b)], whose related $\delta_l(\sigma)$ function almost coincides with the experimental phase shift, appears much more realistic. In this case, the relevant singularities lie outside analyticity parabolas $\mathcal{P}(\mu^2)$ corresponding to reasonable ranges for the interaction.

Type III [Figs. 1(c) and 2(c)] seems less satisfactory since the related singularities lie generally just near or even slightly inside the parabola $\mathcal{P}(4)$. But in this case, one can argue that these singularities, which concern a relatively high-energy region, also simulate some inelastic cuts lying on the positive real axis. On the other hand, in the low-energy region the related $\delta_l(\sigma)$ function agrees with the experimental phase shift, and this type, like the preceding one, seems to be associated with rather reasonable attractive forces.[27]

Let us remark for completeness that, whatever the type of $g_l^2(p)$, the functions $[D_l(\sigma)]^{-1}$ appear well represented in the vicinity of $\sigma = \sigma_r$ by essentially the same Breit-Wigner formula, except for a normalization factor which depends on c. For convenience we have imposed on all these functions the condition

$$[D_l(\sigma_r)]^{-1} = i\,\mathrm{Im}[D_l(\sigma_r)]^{-1} = i/\rho(\sigma_r)$$

[see Eq. (2.12) for the definition of $\rho(\sigma)$], which gives rise to the curves of Fig. 3. With this convention all the $g_l^2(p)$ satisfy $g_l^2[p(\sigma_r)] = 1$ [remember Eq. (3.8) with $\delta_l(\sigma_r) = \pm\frac{1}{2}\pi$] and have nearly the same small derivative at $\sigma = \sigma_r$, as is taken into account in Figs. 1. Clearly the domain of σ values where these two properties remain valid is more or less extended according to the position of the singularities of $g_l^2(p)$. So, the $g_l^2(p)$ of type II remain flat because these singularities are removed far away from the physical region. On the con-

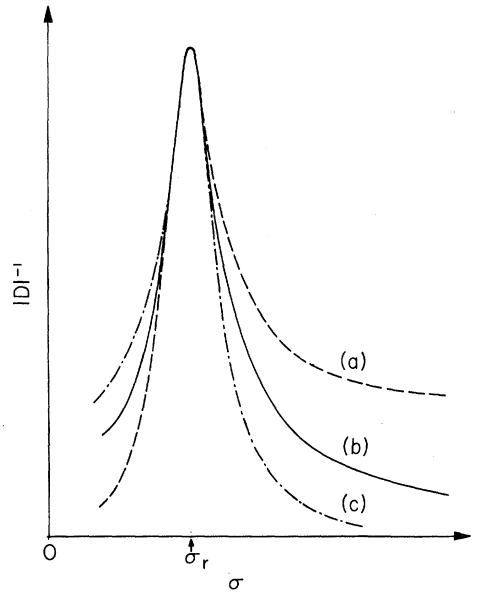

FIG. 3. The $|D|^{-1}$ functions corresponding to the three g_l^2 factors of Fig. 1. The ordinate unit is such that their common maximum value equals unity.

trary, the $g_l^2(p)$ of types I and III possess sizeable enhancements near the values $\sigma_r' \neq \sigma_r$ where $\delta_l(\sigma)$ crosses $\pm\frac{1}{2}\pi$ again. As a consequence, for a given value of n, the area delimited by the $g_l^2(p)$ and the real axis, i.e., the mean value of the $g_l^2(p)$, is generally larger for these two types. To obtain comparable mean values with $g_l^2(p)$ of type II, we must indeed let them decrease slowly at infinity, i.e., take n small or c nearly equal to zero.

C. Numerical Treatment

All the functions $g_l^2(p)$ and $D_l(\sigma)$ which have been retained in the calculations are such that Eqs. (3.3) are of the Fredholm type. The predictions of the model concerning the three-body resonances are then obtained by studying the Fredholm determinant $\mathfrak{D}(\sqrt{s})$ and the eigenvalues associated with these equations. Remember that the three-body resonance poles lie on an unphysical sheet reached as indicated in Fig. 4. At such points one of the eigenvalues becomes equal to unity, and correspondingly $\mathfrak{D}(\sqrt{s})$ vanishes.

The numerical treatment of the integral equations (3.3) is, however, greatly complicated by the presence of moving logarithmic singularities in the kernels. Several recipes have been used to overcome these difficulties.[28] Our own experiment in another approach of the three-body problem[24,25] has led us to follow as often as possible a method first applied to the Faddeev equations by Hetherington and Schick and by Barbour and Schult.[29] The main trick consists in replacing the integration path by another equivalent one which can be easily parametrized and which lies far enough from the singularities of the integrand. By doing so, fewer mesh points are needed for the numerical integration. In the present problem, it is sufficient to turn the q' contour of Eq. (3.3) into the lower-half complex plane as is done in Ref. 29. [The asymptotic behavior of $g_l(p)$ guarantees the validity of the transformation.] By keeping at the same time the variable q on the same contour this is sufficient for our purpose – we can so rotate it without distortion as long as no singularity of the integrand is reached. This is not a very restrictive condition if $g_l(p)$ only possesses real left-hand singularities [as in the representations (3.6) and (3.6′)]. As is well known, the interest of the procedure is, however, greatly restricted when $g_l(p)$ possesses complex poles on both sides of the positive real q' axis.[29]

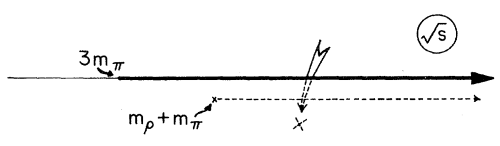

FIG. 4. The $\sqrt{s}$ analytic continuation needed for locating the three-body resonance poles in the $\pi\pi\pi$ case.

In practice, we generally proceed in two steps. In the first one, we try to obtain information about the existence of the three-body resonances by remaining on the physical sheet of the $\sqrt{s}$ variable. This needs no new transformation of Eq. (3.3). Afterwards, provided that the path of integration can be sufficiently rotated, we perform a direct search for the three-body resonance pole by going on an unphysical sheet as shown in Fig. 4.

In all cases we begin thus by plotting both the variations of the largest eigenvalue $\bar{\lambda}(\sqrt{s})$ of K/D and the variations of $|\mathfrak{D}(\sqrt{s})|^{-2}$ when $\sqrt{s}$ runs along a parallel to the real axis. The distance $\mathrm{Im}\sqrt{s} \geq 0$ is suitably chosen to allow at the same time a reasonably good numerical integration; it is taken equal to zero when the q' contour in Eq. (3.3) can be rotated. Note that the interest in considering $\bar{\lambda}(\sqrt{s})$ instead of the largest eigenvalue $\lambda(\sqrt{s})$ of the full kernel $\alpha CK/D$ is that $\bar{\lambda}(\sqrt{s})$ does not depend on the isospin and G-parity coefficients: The curves $\bar{\lambda}(\sqrt{s})$ versus $\sqrt{s}$ can thus be used for examining several $\mathcal{J}^G$ states at the same time.

The presence of a three-body resonance is revealed in this way by a bump in $|\mathfrak{D}(\sqrt{s})|^{-2}$. Also, the difference

$$\mathrm{Re}\bar{\lambda}(\sqrt{s}) - [\alpha C(\mathcal{J})]^{-1}$$

[or equivalently $\mathrm{Re}\lambda(\sqrt{s}) - 1$] takes its smallest

values. At the same time, $|\mathrm{Im}\bar{\lambda}(\sqrt{s})|$ is small and the product

$$[d\,\mathrm{Re}\bar{\lambda}(\sqrt{s})/d\sqrt{s}\,]\,\mathrm{Im}\bar{\lambda}(\sqrt{s})$$

is positive.

It happens that in almost all the cases of interest, the variations of $\bar{\lambda}(\sqrt{s})$ present a typical dispersive form which enables one to fit the curve $[\bar{\lambda}(\sqrt{s})]^{-1}$ by the linear development

$$[\bar{\lambda}(\sqrt{s})]^{-1}=\beta\sqrt{s}-\gamma, \tag{3.12}$$

where β and γ are two complex parameters. Correspondingly, $|\mathfrak{D}(\sqrt{s})|^{-2}$ is rather well represented by

$$|\mathfrak{D}(\sqrt{s})|^{-2}\simeq\left|\frac{A}{1-\alpha C(g)\bar{\lambda}(\sqrt{s})}\right|^2$$

$$=\left|\frac{A}{1-\alpha C(g)/(\beta\sqrt{s}-\gamma)}\right|^2, \tag{3.13}$$

where the constant A stands for the contribution of the smaller eigenvalues. The extrapolation of the two formulas (3.12) and (3.13) enables one to determine the position of the resonance poles with a rather good precision when the resonance is not too broad.

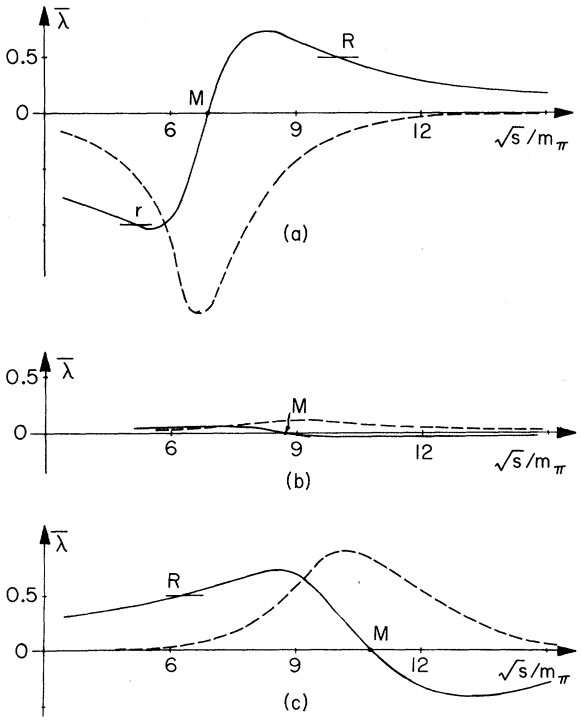

FIG. 5. The plots of the largest eigenvalue $\bar{\lambda}$ versus $\mathrm{Re}\sqrt{s}$ obtained with the three g_l^2 factors of Fig. 1 in the $J^P=1^-$ ($g=0$) $\pi\pi\pi$ case ($\mathrm{Im}\sqrt{s}=0.4m_\pi$). The solid curve is the real part, the dashed curve the imaginary part.

D. Influence of the Form Factors

The above procedure has been applied for different $g^G(J^P)$ values and for different types of form factors $g_l(p)$.

Let us first look at the variations of the results with respect to the latter.

This can be conveniently studied by varying continuously the free parameter c in the expansion (3.9). By so doing, we generally observe a close relationship between the variations and the size of the eigenvalues $\bar{\lambda}(\sqrt{s})$ and $|\mathfrak{D}(\sqrt{s})|^{-2}$ and that of the mean value of the factor $g_l^2(p)$, or $\bar{g}_l^2(p)=p^{-2l}g_l^2(p)$. This is already illustrated by the three curves of Fig. 5 obtained in the $g^G(J^P)=0^-(1^-)$ $\pi\pi\pi$ case with the $g_l^2(p)$ shown[30] in Fig. 1. The fact is indeed not very surprising for one might have expected *a priori* that the larger the magnitude of $\bar{g}_l(p)$ over the integration domain ($|D|^{-1}$ is nearly the same for the different two-body amplitudes; see Fig. 3), the larger the kernel of the three-body equations and the larger the eigenvalues. (Note however that the effects of other factors or constraints like unitarity might have changed this assertion.) This explains why eigenvalues of sufficiently large magnitude – that is here, whose real part is nearly equal to unity (see Sec. III C) – are observed essentially for c values near the points $c=c_0$ or $c=0$ where the mean values of the $g_l^2(p)$ become also sufficiently large (see the end of Sec. III B).

Still starting from Eq. (3.9), we have also tried to understand how the three-body results depend on the detailed properties of the factors $g_l^2(p)$, in particular near the c values leading to large eigenvalues, and which therefore are the most interesting ones for our purpose.

A first possibility is then to take c nearly equal to c_0. In this case, a careful examination of the expression (2.15) shows that the existence of a sharp low-energy peak in g_l^2 or $\bar{g}_l^2$ (this becomes sharper and closer to the two-body threshold when c tends towards c_0) makes the diagonal elements of the K matrix the most important. Moreover, one can show that $\mathrm{Re}K(q',q')$ [$\mathrm{Im}K(q',q')$ is smaller] presents a peak at small (nonrelativistic) q' values, i.e., near $\sigma=(\sqrt{s}-m)^2$ [see Eq. (2.4)]. An insight into the properties of the eigenvalues of the kernel K/D is thus obtained by considering

$$\mathrm{Tr}(K/D)=\int_{-\infty}^{(\sqrt{s}-m)^2}d\sigma'\frac{dq'}{d\sigma'}\frac{1}{D(\sigma')}K(q'(\sigma'),q'(\sigma')). \tag{3.14}$$

The variations of this quantity with respect to $\sqrt{s}$

can be estimated by looking at the relative position of the peaks and zeros of $Kdq'/d\sigma'$ and $1/D$. In particular, one can roughly predict that the imaginary part of $\mathrm{Tr}(K/D)$ becomes maximum (at the same point the real part vanishes) when $\sigma_m = \sigma_r$ with σ_m (σ_r) the position of the maximum of $\mathrm{Re}K(q', q')$ ($\mathrm{Im}[1/D(\sigma')]$). As σ_m lies near $(\sqrt{s} - m)^2$, one thus understands why the point M in Fig. 5(a) lies near the particle + resonance threshold ($\sqrt{s} = m + \sqrt{\sigma_r}$) as shown by the complete numerical treatment. On the other hand, the numerical calculations show that the positions of the three-body resonances are rather stable with respect to a change of n or c in Eq. (3.9) (the stability of their widths is less satisfactory). This may be also understood qualitatively by noticing that neither the position of the peak of $g_l^2(p)$ or $\bar{g}_l^2(p)$ [this peak remains between the threshold and σ_r; see Fig. 1(a)] nor the position of the corresponding peak of $K(q', q')$ in $\mathrm{Tr}(K/D)$ [Eq. (3.14)] drastically changes. Thence the curve $\bar{\lambda}(\sqrt{s})$ and the position of the bump of $|\mathfrak{D}(\sqrt{s})|^{-2}$ remain rather stable.

A second possibility for observing large eigenvalues is to take c nearly equal to zero in Eq. (3.9). In this case, the largest contribution of the kernel $K(q', q')$ in $\mathrm{Tr}(K/D)$ [Eq. (3.14)] comes from high (relativistic) values of q'. This enhancement in $K(q', q')$ is, however, generally much broader than the peak observed for c near c_0, which makes more difficult any interpretation of the main features of Fig. 5(c) in terms of K and $1/D$ contributions. One can nevertheless argue that this enhancement is still again closely related to that of $g_l(p)$. As the latter which can now vary between σ_r and ∞, the former is very sensitive to variations of the parameters n and c. This, with the help of Eq. (3.14), explains why the three-body results are much less stable than in the preceding case $c \simeq c_0$. In particular, for a given n, the location of the three-body resonances may be very dependent on the value of c. The latter has therefore to be chosen in order to fit one of the experimentally best established three-body resonances, after which predictions on the other $\mathcal{G}^G(J^P)$ resonant states can be made.

This discussion reveals that, besides the $1/D$ resonance pole, the detailed properties of the $g_l^2(p)$ may play an important role in the types of calculations performed here or in similar preceding works.[9,10] As the relevant peculiarities of the $g_l^2(p)$ either concern energy regions on which we have little information or even appear unjustified, as, e.g., the low-energy peak of the $g_l^2(p)$ of type I, the reliability of the corresponding three-body results may be therefore somewhat doubtful.

This leads us naturally to return to the discussion of Sec. III B about the ability of each type of $g_l^2(p)$ in Fig. 1 to represent the physical situation.

In this context, the apparently more realistic two-body amplitudes to be used are of type II [Fig. 1(b)]. Unfortunately the corresponding three-body results appear rather disappointing. First, large eigenvalues with $\mathrm{Re}\bar{\lambda}(\sqrt{s}) \simeq 1$ can occur in this case only if large contributions from the rather unknown high-energy part of the integration are included (n must be taken small or $c < 0$ nearly equal to zero). This is one negative aspect, although the possibility of such contributions is not excluded in the problem (a discussion about their possible significance is reported in Ref. 25). More inconvenient is the fact that the variations and the signs we then generally observe for $\mathrm{Re}\bar{\lambda}(\sqrt{s})$ and $\mathrm{Im}\bar{\lambda}(\sqrt{s})$ are not compatible with the existence of three-body resonant states of positive width [they are such that the product $d\,\mathrm{Re}\bar{\lambda}(\sqrt{s})/d\sqrt{s}$. $\mathrm{Im}\bar{\lambda}(\sqrt{s})$ is negative; cf. Sec. III C]. This result differs from that observed elsewhere with a dispersive on-shell model in which the ω, for instance, can be found under these conditions.[25] This discrepancy might be due, among other reasons, to the effects of the extra singularity at $\sqrt{s} = 0$ encountered in the present model.[10]

Finally, true three-body resonances have been observed in the present calculations essentially with type I ($c \lesssim c_0$) and type III ($c > 0$). Owing to the discussions of Sec. III B, it seems natural to consider as the more reasonable and the more acceptable ones, the results obtained with the $g_l^2(p)$ of type III whose behavior above σ_r furthermore provides a convenient cutoff in the high-energy region. These will be mainly taken into account in what follows. Although their physical meaning is more questionable, the results deduced with choice I will be nevertheless also mentioned for comparison. Indeed, the tables will show that among the three-body resonances obtained in this case, one series possesses the same quantum numbers as those observed with choice III. Taking into account the above discussion of $\mathrm{Tr}(K/D)$, we see that this mainly follows from a certain symmetry between the properties of the two-body amplitudes of types I and III with respect to the two-body resonant mass σ_r: According to the type, the peak of the $g_l^2(p)$ and the point where $\delta_l(\sigma)$ crosses $\pm\frac{1}{2}\pi$ again are encountered on one or the other side of σ_r (see Fig. 1). This gives rise to a correspondence between the signs and variations of $\mathrm{Re}\bar{\lambda}(\sqrt{s})$ and $\mathrm{Im}\bar{\lambda}(\sqrt{s})$, which allows one to predict with some accuracy in which quantum numbers three-body resonances can occur for one type, once they are known for the other. We shall take for granted this mainly mathematical property in Sec. IV when using the type-I amplitude which in other respects allows the easiest calculations.

TABLE II. Masses and widths in MeV of the resonances obtained in the $\pi\pi\pi$ case. The quoted numbers are rounded to 50 MeV and the too broad enhancements are not reported. When they are sufficiently different, two sets of values are reported for the main resonances printed in italic in Table II(a): The first one is associated with the inverse squared Fredholm determinant, the other (in parentheses) with the position of the true resonance pole on the unphysical sheet.

	$\mathcal{I}=0$		$\mathcal{I}=1$ and 2	
J^P	M	Γ	M	Γ
		(a)		
0^-	500	< 100	*1250*	*250*
			(1050)	*(200)*
1^-	*1450*	*150*	500	< 100
1^+	500	100	*1150*	*200*
			(1050)	*(150)*
2^-	500	< 100	*1300*	*300*
			(1050)	*(200)*
2^+	500	150	*1200*	*<300*
			(1150)	*(350)*
		(b)		
0^-			*1050*	*<100*
1^-	*850*	*<50*	2000	300
1^+			*1050*	*150*
2^-			*1100*	*150*
2^+			*1400*	*<250*

TABLE III. Masses and widths in MeV of the resonances obtained in the $\mathcal{I}=0$ $K\bar{K}\pi$ case. The conventions are the same as in Table II.

	$G=-1$		$G=+1$	
J^P	M	Γ	M	Γ
		(a)		
0^-	1350	100	*1650*	*150*
1^-	*1650*	*<100*	1250	< 50
1^+	1150	50	*1550*	*<100*
	1200	50		
2^-	1300	50	*1700*	*<250*
2^+	1300	50	*1600*	*100*
	1200	50		
		(b)		
0^-	2200	200	*1400*	*<50*
1^-	*1500*	*<50*		
1^+			*1450*	*<50*
2^-			*1400*	*<50*
2^+			*1950*	*150*

E. Comparison with Experiment

The results obtained with type I are given in Tables II(a) ($\pi\pi\pi$ case) and III(a) ($K\bar{K}\pi$ case) [the quoted values[31] have been more precisely deduced with the representation (3.6) and (3.6′)]. Those observed with type III are given in Tables II(b) and III(b). Table II(b) concerns the $\pi\pi\pi$ case and has been obtained with the representation (3.10). The free parameter c – the same for all J – has been chosen in the related representation (3.9) in order to nearly give the masses of the better established A mesons. Table III(b) concerns the $K\bar{K}\pi$ case[13] and has been obtained by choosing c in order to nearly fit the mass (1420 MeV) of the E meson.[18]

In what follows all the values quoted in these tables are however not treated on an equal footing. First, there are in Tables II(a) and III(a) low-mass resonances which are related to the low-energy part of the curves $\bar{\lambda}(\sqrt{s})$ [i.e., to the point r in Fig. 5(a)]. These, owing to the remarks of the preceding section, are only quoted for completeness and are printed in small roman type.[32] Similarly, in Tables II(b) and III(b), there are high-mass resonances which correspond to the high-energy part of the curves $\bar{\lambda}(\sqrt{s})$ in Fig. 5(c). Probably several inelastic effects can change their characteristics, and moreover the present numerical treatment does not enable one to determine them with a sufficient accuracy. The few which are reported are therefore also printed in small roman type.

Our attention has been mainly focused on the intermediate-energy resonances which are printed in italic type in the tables: They correspond to the highest-energy part of $\mathrm{Re}\bar{\lambda}(\sqrt{s})$ in Fig. 5(a) and to the lowest-energy part in Fig. 5(c) (i.e., to the point R in these figures). In Table II(a), they are generally characterized by two sets of values. The first one follows from the examination of $|\mathfrak{D}|^{-2}$; the second one (in parentheses) gives the position of the nearest resonance pole which can be specified in this case by rotating the q' path in Eq. (3.3) (only the first set is reported when the difference between the two is small, as is the case for a sharp resonance). One may ask which of the two sets can the most truly represent the experimental information: Probably a thorough analysis of the latter would also require the calculation of the Fredholm numerator of Eq. (3.3), or at least the calculation of the most important eigenfunctions. In Tables II(b), III(a), and III(b), only information deduced from the consideration of $|\mathfrak{D}(\sqrt{s})|^{-2}$ on the real axis is reported with, if necessary, the help of formula (3.13).

1. *The Three-Pion System*

The $\mathcal{I}=1$ and $\mathcal{I}=2$ resonances. The two isospin states $\mathcal{I}=1, 2$ are degenerate in the present model. To break up this degeneracy it would be necessary either to include other $\pi\pi$ effects such as the low-energy $I=0$ enhancement, or the f_0, or to take account of other channels such as the $K\bar{K}$ or $K\bar{K}\pi$ sys-

tems[33] (the latter is here studied independently). As already noticed elsewhere,[10] the conservation laws imply that many of these new effects do not contribute to the $g=2$ channel, to which our results therefore mainly apply, for representing the true $\pi\pi\pi$ situation.

Tables II(a) and II(b) indicate resonances in the $J^P=0^-$, 1^+, 2^-, and 2^+ states.[32] No experimental report seems to concern the $g=1$ (or $g=2$) 0^- object. But the 1^+ and 2^- candidates (despite their large widths) may be associated with the A_1(1080 MeV) and the $A_{1,5}$(1180 MeV) mesons whose existence seems compelled by works like those reported in Ref. 19. The 2^+ peak might correspond as well to the A_2(1300 MeV) meson whose existence seems now beyond any doubt, as to the eventual 1320-MeV $g=2$ $\rho^-\pi^-$ object.[34] However, we must specify that the 2^+ enhancement appears as very broad and scarcely distinguishable in the present calculations. Perhaps the coupling with another channel might reinforce this bump and explain its possible splitting into narrower resonances[35,36] as observed in several experiments.[19] The $K\bar{K}$ channel seems of particular importance in this respect: First, the $K\bar{K}$ system is found in the decay products of the A_2; next, recent two-body calculations give evidence for a $K\bar{K}$ resonance in the 1300-MeV region.[37]

The $g=0$ resonances. With the form factors of type I, small and ill-defined enhancements, which are not mentioned in Table II(a), are observed in the 1^+ and 2^- states. Indeed in these two states, the integral equations (3.3) are coupled, and generally several important eigenvalues are found. The most important one gives rise to the above $g=1, 2$ resonances, and the second one to the $g=0$ small enhancements.

The 1^- state deserves more attention. In addition to the 1450-MeV object of Table II(a) already mentioned in Ref. 9, one indeed finds in Table II(b) a resonance which possesses almost all the characteristics of the ω meson.[33,38] Although near this low-mass resonance the reliability of our calculations can be still more questionable than at higher energies,[10] this agreement with experiment is somewhat satisfactory since it happens in an $g^G(J^P)$ state and in a region where our approximation of keeping only one $\pi\pi$ wave ($I=1$, $l=1$) in the problem can be best justified.

2. *The $K\bar{K}\pi$ System*

Remember that in the present approach, the $\pi\pi\pi$ and $K\bar{K}\pi$ systems are both described by the same type of integral equations (3.3). This means that if we neglect in a first step the difference between the masses of the K and π particles and between the characteristics of the K^* and ρ resonances, we can as well examine the $K\bar{K}\pi$ resonances with the help of the curves $\bar{\lambda}(\sqrt{s})$ drawn in Figs. 5 for the $\pi\pi\pi$ case. The only new parameters are then the coefficients $\alpha C(g)$. This is precisely what we should have assumed in an SU(3)-invariant formalism. Under these simplifying assumptions, a $K\bar{K}\pi$ resonance is thus expected every time that a $\pi\pi\pi$ resonance is observed, provided that the coefficients $\alpha C(g)$ are nearly the same in both cases. The $\pi\pi\pi$ and $K\bar{K}\pi$ $g^G(J^P)$ states which can be so put into correspondence[13] are easily found by comparing Tables I(a) and I(b). From the results of Tables II(a) and II(b), we can therefore expect the $K\bar{K}\pi$ resonances to occur in the following states: $0^+(0^-)$, $0^+(1^+)$, $0^+(2^-)$, $0^+(2^+)$, and $0^-(1^-)$. Note moreover that the coefficients $\alpha C(g)$ corresponding to the isospin $g=1$ are one-third those corresponding to $g=0$. As a consequence, with each $g=0$ $K\bar{K}\pi$ resonance may be associated an $g=1$ object which may be expected to have a larger width, to be less easily distinguishable and displaced towards the maximum of $\mathrm{Im}\bar{\lambda}(\sqrt{s})$ in Figs. 5(a) and 5(c).

Now, we must superimpose on these predictions the effects of the differences of masses and widths, which can be thoroughly estimated only after the complete numerical treatment of Eq. (3.3). This yields the results quoted in Tables III(a) and III(b). For simplicity, we have given only the $g=0$ resonances in these tables, it being implicitly understood, as just discussed above, that correspondingly resonances may occur in the $g=1$ isospin. Precisely, the experimental evidence for an $g=1$ (1540 MeV) $K^*\bar{K}+\bar{K}^*K$ resonance (the F_1) has been reported.[19]

We observe that in both Tables III(a) and III(b) all the $K\bar{K}\pi$ resonances predicted from the $\pi\pi\pi$ case are present, but have a higher mass. At the same time, the enhancements in the $K\bar{K}\pi$ case are much sharper and more easily distinguishable than in the $\pi\pi\pi$ case. This seems mainly due to the narrower width of the K^* compared to the ρ.[9,39] Note also that because of parity and G-parity conservation the results in the $G=+1$, $J^P=1^-$ and 2^+ and in the $G=-1$ [Eq. (3.2′)] states cannot be affected by the inclusion of the $K\bar{K}$ enhancement if this as believed is $I=1$, $l=0$.

The $G=+1$ resonances. Almost all the experimentally observed $K\bar{K}\pi$ resonances have $G=+1$, as the E(1420 MeV) and the D(1285 MeV) mesons. Both Tables[32] III(a) and III(b) offer four candidates[13] which have again $J^P=0^-$, 1^+, 2^-, and 2^+. Remember that in Table III(b), the 0^- enhancement has been associated with the E meson by choosing c in Eqs. (3.9)–(3.10) consequently. Note, however,

that 1^+ does not seem completely excluded for this resonance and that the neglected $K\bar{K}$ enhancement is 50% observed in the E decay products.[40] Our choice of c might thus not be the most adequate[33]; in fact, a displacement of the 0^- peak could decrease the rather too great masses of the 1^+ and 2^- candidates that we should have been tempted to associate (especially the first) with the D meson. But still more in this case the neglect of the $K\bar{K}$ interaction might be an irrelevant approximation [the $\pi(K\bar{K})_{I=1}$ decay mode of the D meson is predominant].[40] Lastly, many of the difficulties which were encountered in the 2^+ $\pi\pi\pi$ case appear here again when we try to compare the 2^+ candidate of Table III(b) with the experimentally observed f'(1515 MeV). But one can state that the two-body $K\bar{K}$ decay mode of the f' is largely predominant and that there is only a weak indication for a $K^*\bar{K}+\bar{K}^*K$ decay mode[19] (the f' is also found in the calculations of Ref. 37).

The $G=-1$ resonances. These resonances may *a priori* also decay into three pions and should be therefore more thoroughly studied by considering the two $\pi\pi\pi$ and $K\bar{K}\pi$ systems simultaneously (see for instance Ref. 36). The only important resonance which is obtained in the present model is a 1^- object for which no experimental evidence seems yet to have been noticed.

F. Further Remarks and Discussions

In Sec. III D, we began with a discussion about the influence of the mean value of the form factor $g_l(p)$ on the three-body results. As examined elsewhere,[25] this indeed provides a particular example of the effects of the strength of the $\rho\pi$ potential, which depends on the ρ-$\pi\pi$ coupling and consequently on the mean value of the two-body amplitude (see another example in footnote 39).

But of course these quantities alone are not sufficient to explain all the observed results. An example which shows that the detailed shape of the two-body amplitude is also of some importance appears by comparing Tables II(a) and II(b). In both cases, large mean values of the $g_l^2(p)$ and thus large $\lambda(\sqrt{s})$ as well as three-body resonances can be found in the $0^-(1^-)$ state. However, in the case of Table II(a) [type I of $g_l^2(p)$], it was not possible to put the resonance mass in coincidence with that of the ω meson because of inconsistencies with the sign of $\mathrm{Im}\lambda(\sqrt{s})$. This sign is indeed closely related to the two-body scattering length[25] which is somewhat unrealistic for type I.

In other respects, it was also shown in Sec. III D that for some choices of the two-body amplitude the bumps of the related $g_l^2(p)$ may play an important role. These indeed reveal the existence of nearby singularities and one can now try to reinterpret many of the conclusions given in Sec. III D in terms of the effects they induce in the three-body results.

More generally, one can ask which singularities and which related mechanisms may be at the origin of the main features described above, for instance the typical dispersive form of the curves $\lambda(\sqrt{s})$ and $\mathfrak{D}(\sqrt{s})$ [see Figs. 5(a) and 5(c)] for some choices of the two-body amplitudes. We have two sources of information for answering this question.

On the one hand, general considerations on the analytic properties of the kernel K of Eq. (3.3) as well as on its trace [Eq. (3.14)] can give an insight into the main analytic structure of the eigenvalues and of $\mathfrak{D}(\sqrt{s})$. Two sets of singularities may then be expected to play a role in the problem. First there are the three-body threshold, the particle + resonance threshold, and the so-called Peierls singularities[41] induced by the singularities of the Green's function and of the $1/D$ part of the two-body amplitude. Next there are singularities resulting from those of the form factors $g_l(p(\sigma))$. A singularity σ_0 of the latter generates among others an end point singularity in $K(q', q')$ which by pinching with the resonance pole of $1/D$ in Eq. (3.14) yields singularities at

$$\sqrt{s} = \omega_0 \pm (\omega_0^2 - m^2 + \sigma_r)^{1/2} \tag{3.15}$$

with

$$\omega_0 = \frac{\sigma_0}{2m} - m$$

or

$$\omega_0 = \frac{\frac{1}{2}\sigma_0 + m^2}{(2\sigma_0 + m^2)^{1/2}}$$

(these formulas concern the three-pion case with $m = m_\pi$). As one can verify, many of these singularities can directly communicate with the physical sheet, in contrast with the Peierls singularities which are generally hidden by the resonance + particle cut. They can, moreover, lie near the physical boundary when the singularities of g_l lie near the physical region.

On the other hand, there are the results of the present calculations which are well represented through Eq. (3.13) and which show that at the end of the numerical treatment all the expected singularities are nearly equivalent to a single pole at $\sqrt{s} = \gamma/\beta$.

The problem is then to disclose some relationship between the equivalent pole and one particular singularity which can thus be considered as predominant. This is in fact a difficult task because several singularities can lie in the same neighbor-

hood of the Riemann sheet and the weight of each singularity (i.e., the discontinuity across the corresponding cut) generally depends on complicated factors. A natural way to proceed is to vary a parameter of the model on which only a few of the main singularities can be reasonably assumed to depend.

Among these parameters, there is the coefficient c in (3.9) which affects the position of the singularities induced by the g_l (note that the other main singularities do not – or scarcely – depend upon this parameter, but their weights do). By varying c, one can therefore hope to disclose the effects of such singularities which may be expected to play an important role according to the discussions of Sec. III D. By so doing, we find effectively that over large domains of c values, the position of the equivalent pole $\sqrt{s} = \gamma/\beta$ is essentially determined by that of one of the singularities (3.15). Many of the remarks in Sec. III D about the dependence of the curves $\bar{\lambda}(\sqrt{s})$ on the details of $g_l(p)$ can even be reinterpreted by simply identifying γ/β with such a singularity. [Predictions for $|\mathfrak{D}|^{-2}$ are less easily obtained since Eq. (3.13) depends moreover on the weight of this singularity.] This is especially true for c near c_0 (i.e., for g_l factors of type I) in which case one singularity (3.15) lies very near the resonance+particle threshold. A similar correspondence is also found for $g_l(p)$ factors of type III having singularities not too far from the physical region.

These remarks confirm the importance and even the dominance, for some choices of the two-body amplitudes, of the effects induced by the factors $g_l^2(p)$. As discussed in Sec. III D, this can make rather questionable the physical meaning of the related three-body results, since the relevant peculiarities often reveal some unrealistic or unreliable properties of the associated two-body forces.

At the same time this seems to leave no possibility for easily observing the effects of the resonance-plus-particle threshold and of the Peierls singularities.[41] Many results nevertheless show that the former may play a role which, if not dominant, is revealed by the fact that $\mathrm{Im}\bar{\lambda}(\sqrt{s})$ becomes mainly sizeable for s values greater than $(\sqrt{\sigma_r} + m_\pi)^2$. But no definite information has been obtained concerning the latter. One might think that both effects could be better analyzed with form factors of type II [Fig. 1(b)], whose singularities lie far away from the physical region and thus can be expected to induce small effects. But in this case the present calculations show that the eigenvalues are then generally small, unless the convergence of the integral at infinity is decreased, in which case they appear mainly dominated by a slowly varying background associated with very-high-energy contributions.

The mass of the two-body resonance provides another parameter that can be conveniently varied, as first done in Refs. 9 and 10 with the type-I representation (3.6), which is completely determined from the characteristics of the two-body resonance. Our results in this case indeed still again disclose the dominance of one of the singularities (3.15) which remains near the resonance-plus-particle threshold and also behaves like $\sqrt{\sigma_r}$ for large σ_r. The method is of less interest for choice III of form factors because, in this case, the result might be very dependent on how the parameter c is simultaneously chosen (see Sec. III D).

Also, for this reason, the procedure does not enable one to clearly disclose any correspondence between the masses of the resonances quoted in Tables II(b) and III(b) and that corresponding to a simultaneous overlap of the two-body resonant bands in the Dalitz plot.[10,42] At this stage, two simple conclusions can nevertheless be drawn about this subject:

(1) In the present approach, three-body resonances can obviously be obtained when only two of the three pairs of particles can resonate. This is in fact what happens for the $K\bar{K}\pi$ system, where the neglect of the $K\bar{K}$ interaction makes the notion of the three-band intersection meaningless.

(2) However, had we neglected the effect of one resonant pair of pions in the study of the $\pi\pi\pi$ system, we should have cut the same curves $\mathrm{Re}\bar{\lambda}(\sqrt{s})$ as before by the straight line $[C(\mathcal{J})]^{-1}$ instead of $[2C(\mathcal{J})]^{-1}$. The peculiar dispersive forms of these curves [Figs. 5(a) and 5(c)] show that the resulting three-body resonances are shifted towards highest $\mathrm{Im}\bar{\lambda}(\sqrt{s})$ values. As a consequence, their widths become larger and the bumps in $|\mathfrak{D}|^{-2}$ less important. In this case, *the three resonant pairs interfere thus constructively*. We cannot, however, argue that this is a general feature for three-body reactions. In the following section, the $K\pi\pi$ system will indeed offer us simple examples of *destructive* interferences.

IV. $K\pi\pi$ SYSTEM

A. Equations

The $K\pi\pi$ system[14] appears experimentally dominated over a large domain of energy by the effects of the ρ and the K^*, two types of resonances which have been considered separately in Sec. III. This case provides thus the best field for a simple extension of the preceding results to three-body systems in which several types of two-body reso-

nances are simultaneously involved. Note also that because of parity conservation only the results in the $J^P = 1^-$ and 2^+ states may be affected by the coupling with the two-body $K\pi$ channel.

The integral equations follow from Eq. (2.15) and from the symmetry conditions imposed by Bose-Einstein statistics which read in this case

$$B_{2I}^{\Lambda I}(q) = (-)^{I+I-\tau_\pi-\tau_K} B_{1I}^{\Lambda I}(q) \tag{4.1}$$

and

$$B_{3I_3}^{\Lambda 3 I_3}(q_3) \equiv 0 \quad \text{unless } l_3 + I_3 \text{ even} \tag{4.1'}$$

with

$$l = l_{K^*} = 1, \quad I = I_{K^*} = \tfrac{1}{2}, \; l_3 = l_\rho = 1, \quad I_3 = I_\rho = 1$$

(the index 3 labels the $\pi\pi$ channel). We can get rid of the coupling through channel indices by one iteration [$B_{3I_3}^{\Lambda 3 I_3}$ is replaced by its integral expression in terms of $B_{1I}^{\Lambda I}$ and $B_{2I}^{\Lambda I}$]. This leads finally to

$$B^{\Lambda}(q) = B_0^{\Lambda}(q) + C_{II}(\mathcal{I}) \frac{1}{D(\sigma)} \sum_{\Lambda'=0,1} \int_0^\infty dq' \, {}_1^{\Lambda}K_2^{\Lambda'}(q, q') B^{\Lambda'}(q')$$

$$+ 2C_{II_3}(\mathcal{I}) C_{I_3 I}(\mathcal{I}) \frac{1}{D(\sigma)} \sum_{\Lambda'=0,1} \int_0^\infty dq' \left[\frac{1}{D_3(\sigma_3')} \sum_{\Lambda_3'=0,1} \int_0^\infty dq_3' \, {}_1^{\Lambda}K_3^{\Lambda_3'}(q, q_3') \, {}_3^{\Lambda_3'}K_1^{\Lambda'}(q_3', q') \right] B^{\Lambda'}(q'), \tag{4.2}$$

where the kernels ${}_iK_j$ have the same expressions as in Eq. (2.16). The isospin recoupling coefficients $C_{II}(\mathcal{I})$ and $C_{II_3}(\mathcal{I}) = C_{I_3 I}(\mathcal{I})$ are given in Table IV.

Because of the presence of the double integral term, the numerical treatment of Eq. (4.2) is more difficult and requires more computer time than that of Eq. (3.3). For this reason, we have limited ourselves to the form factors $g_l(p)$ given by Eqs. (3.6) and (3.6') [Fig. 1(a)] enabling one to easily rotate the path of integration and to deal with not too large matrices. From the analysis of Sec. III F, we may hope to obtain in this way some insight into the $\mathcal{I}^G(J^P)$ states in which the most important three-body resonances can be observed. The results regarding the positions and the widths of these resonances are probably more questionable.

Note moreover that the double integral term in Eq. (4.2) is precisely the only one which involves the $\pi\pi$ interaction. By neglecting or including it, we can thus estimate the relative importance of the effects of the K^* and of the ρ resonances.

B. Results

The largest eigenvalue $\lambda(\sqrt{s})$ is shown in Fig. 6 for $J^P = 1^-$, $\mathcal{I} = \frac{1}{2}$. This curve exhibits a typical double dispersive form and appears as a combination of two curves of the type illustrated in Fig. 5(a), one of them being associated with the $K^*\pi$, the other with the $K\rho$ threshold. Of course this is only an example of the possible combinations of two such curves. Other forms may arise, according to the relative value and sign of the isospin coefficients $C_{II}(\mathcal{I})$ and $C_{II_3}(\mathcal{I})$. These various forms clearly illustrate the influence of differences in the masses of the particles, which goes against SU(3) symmetry.

The results regarding three-body resonances can be obtained in two steps. First, we can neglect the second integral term in Eq. (4.2). This approximation leads to a set of resonances which can be put in close correspondence with the results of the $\pi\pi\pi$ and $K\bar{K}\pi$ cases, according to the sign and the magnitude of the coefficient $C_{II}(\mathcal{I})$. [Note also that the same relationship does follow from SU(3) symmetry).] Without further lengthy calculations, we can thus predict bumps in the $\mathcal{I} = \frac{3}{2}$, $J^P = 0^-$, 1^+, 2^-, and 2^+ as well as in the $\mathcal{I} = \frac{1}{2}$, $J^P = 1^-$ states, which is confirmed by a thorough numerical treatment of the truncated Eq. (4.2).

Then the ρ resonance is included. This can give rise to rather different effects according to the

TABLE IV. The isospin coefficients $C_{II}(\mathcal{I})$ and $C_{II_3}(\mathcal{I}) = C_{I_3 I}(\mathcal{I})$ of Eq. (4.2) according to the value of $\mathcal{I}$.

$\mathcal{I}$	$\frac{1}{2}$	$\frac{3}{2}$
$C_{II}(\mathcal{I})$	$\frac{1}{3}$	$-\frac{2}{3}$
$C_{II_3}(\mathcal{I}) = C_{I_3 I}(\mathcal{I})$	$-(\frac{2}{3})^{1/2}$	$-(\frac{1}{6})^{1/2}$

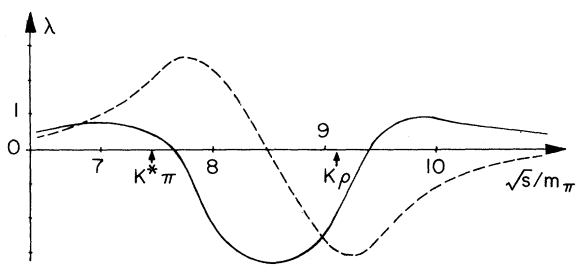

FIG. 6. Plot of the largest eigenvalue λ versus $\sqrt{s}$ in the $J^P = 1^-$ ($\mathcal{I} = \frac{1}{2}$) $K\pi\pi$ case. The solid curve is the real part, the dashed curve the imaginary part.

magnitude and especially the sign of the isospin coefficients. Destructive effects are clearly observed in the $\mathcal{J}=\frac{3}{2}$, $J^P=0^-$ and 2^- states (see Fig. 7): The original large bump in $|\mathfrak{D}|^{-2}$ finally reduces to small enhancements whose observation would probably require many more refinements in the experimental analysis. On the contrary, new bumps appear in the $\mathcal{J}=\frac{1}{2}$, $J^P=1^+$ and 2^+ states and we can argue that in these states there are sizeable three-body resonances only after the insertion of the ρ.

The final results are reported in Table V. The conventions are the same as in Table II(a): The main resonances are written in italic type, and the true resonance pole, when sufficiently different from the position of the bump in $|\mathfrak{D}|^{-2}$, is mentioned in parentheses; the low-energy bumps, associated with the lowest part of the eigenvalue curve, are here again printed in small roman type.

The $\mathcal{J}=\frac{1}{2}$ resonances. The experimental analysis often shows a broad enhancement in the energy region 1.2–1.5 GeV, which is probably due to a combination of a background and of one, two, or more true resonances[43] [namely, the C(1240 MeV) and the K_A(1320 MeV)]. Besides there is the better-known K_N(1420 MeV). Table V also offers candidates in this energy region. Note however that experimentally the decay products of the resonances appear dominated by $K^*\pi$ states while the present analysis indicates a greater influence of the ρ in their production.[40] We must also emphasize that the $K_N(J^P=2^+)$ does not clearly follow from our calculations: This time again we can argue that an important coupling with a two-body system (the $K\pi$ system in this case) might have been neglected. [Note also that the K_N(1420 MeV) is found in the two-body model of Ref. 37.]

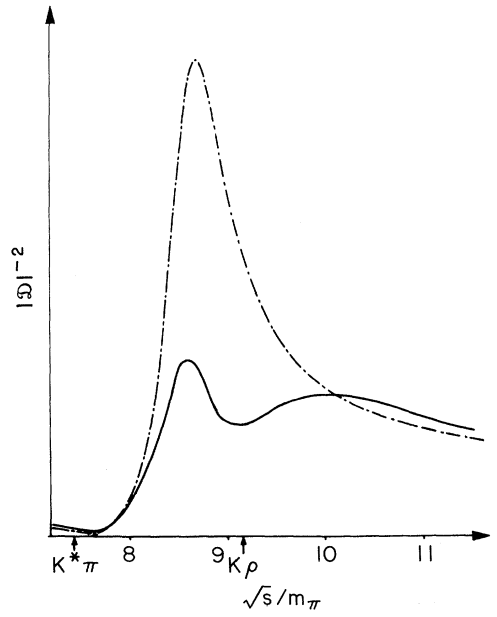

FIG. 7. An example of the destructive interference effects observed in the $K\pi\pi$ case. The dashed curve is $|\mathfrak{D}|^{-2}$ versus $\sqrt{s}$ for $J^P=0^-$ ($\mathcal{J}=\frac{3}{2}$) when only the K^* resonance is taken into account. The solid curve is the final result after the inclusion of the ρ resonance.

The $\mathcal{J}=\frac{3}{2}$ resonances. The experimental evidence of such resonances is not yet compelling. The existences of a 1175- and a 1270-MeV meson have been reported nevertheless in a few works.[43] Table V also indicates three-body resonances in this energy region but we have seen that the corresponding bumps may be small because of destructive interference effects.

V. CONCLUSION

New predictions about three-body resonances have been obtained within the framework of a relativistic extension of the Faddeev equations. Compared to similar preceding works,[9,10] more elaborate numerical techniques as well as less rigid parametrizations of the two-body amplitudes have been used. This allowed for more realistic two-body forces, resulting in a better agreement with experiment which makes more encouraging the use of the model as a tool for investigating the relativistic three-body problem [see Sec. III E and in particular, Table II(b)].[33]

Of course many approximations still remain associated with this approach. On one hand, in the three-body integral equations:

(i) Only the longest-range part of the resonance-particle potential is retained, which can make crossing poorly satisfied; moreover, the "reduc-

TABLE V. Masses and widths in MeV of the resonances obtained in the $K\pi\pi$ case. The conventions are the same as in Table II(a). The $|\mathfrak{D}|^{-2}$ bumps in $J^P=2^+$ are small and broad, so that, correspondingly, no width is given.

	$\mathcal{J}=\frac{1}{2}$		$\mathcal{J}=\frac{3}{2}$	
J^P	M	Γ	M	Γ
0^-	850	150	*1150*	*100*
1^-	*1450*	*<150*	850	100
	850	200		
1^+	*1450*	*200*	900	250
	(1350)	*(100)*		
	850	200		
2^-	850	150	*1550*	*100*
	950	100		
2^+	*1450*		*1400*	
	(1350)	*(<250)*	*(1300)*	*(<250)*

tion procedure" which leads to our basic equations allows one to keep only one part of this potential.

(ii) Three-body forces, in particular the pion pole in the $J^P = 0^-$ state, as well as couplings with other channels are neglected.

On the other hand, as concerns more particularly the two-body input amplitudes:

(i) Only a single wave, $l = 1$, is retained in all J states and over the whole range of energy integration.

(ii) A separable approximation with energy-independent form factors is used, which is mainly justified by simplicity requirements.

It remains that the complexity of the full three-meson problem makes necessary the consideration of such simplified approaches, each one taking into account only some particular aspects of the question. Reasonably, from the comparison of their results there will emerge a more satisfactory picture of the physical situation. In this connection, no elements of comparison are available as concerns the $K\bar{K}\pi$ and $K\pi\pi$ cases. But it is worthwhile to note that for the $\pi\pi\pi$ system many features observed in the present work were also found in an on-shell model based on dispersion relations.[24,25] In the latter, three-body unitarity can be only approximately fulfilled; however, the $\rho\pi$ potential as well as the analytic properties of the three-body amplitudes could be represented in a more satisfactory way. In both models indeed, similar conclusions can be reached about the influence of the parameters related to

(i) the strength of the $\rho\pi$ potential, and in particular the strength of the ρ-$\pi\pi$ coupling which depends on the mean value of the two-body input amplitude;

(ii) the shape of the two-body interaction, namely, its associated singularities, and on the other hand the sign and size of the two-body scattering length on which the characteristics of a low-mass resonance like the ω can be very dependent[25];

(iii) the contribution of the high-energy part of the integrals.

For many of these parameters, especially in the present approach, we however just possess general information of plausibility (see, for instance, the Appendix) which makes some choices more or less realistic. In view of their sensitivity to these rather unknown quantities, the predictions concerning the detailed characteristics of the three-body resonances may be therefore questionable. Nevertheless, a rather good agreement between both models and experiment has been found as concerns the quantum numbers of the states in which the $\rho\pi$ forces associated with the rescattering processes summed up in the equations are "attractive" and in which a three-body resonance can reasonably happen. These last results may therefore be expected to remain valid in more elaborate approaches to the $\rho\pi$ system.

ACKNOWLEDGMENTS

We thank Professor R. L. Omnès and Dr. J. L. Basdevant for suggesting that we look at the $K\pi\pi$ system. We thank also several groups of experimentalists at the Institut de Physique Nucléaire, Paris, and at the Laboratoire de l'Accélérateur Linéaire, Orsay, for discussions.

APPENDIX

The equations satisfied by the two-body off-energy-shell amplitudes involved in the reduced equations (2.1) may be considered as relativistic generalizations of those encountered in nonrelativistic potential theory: They indeed possess the same general structure but also contain convenient kinematic factors warranting relativistic covariance. Correspondingly, the solutions of the two types of equations exhibit similar features which can be conveniently expressed in a given partial wave in terms of analytic properties. For reasons of simplicity, we examine below,[44] as an example, the nonrelativistic case with the methods previously used by one of us[12] (for the complications arising in the relativistic case, see for instance Refs. 20 and 21). The basic potentials are chosen of the Yukawa type[45] because of their close relation with exchange of mass processes usually considered in the relativistic case. This study enables one to better understand the physical meaning of the parameters introduced in Sec. III B.

1. Review of Some Results of Potential Theory

Remember first that it can be shown on rather general grounds[46] that the two-body off-shell partial-wave amplitude $\hat{t}_l(p, P, p')$ exhibits factorization properties with respect to p and p' at the poles in the "on-shell" variable P (here P, p, and p' denote magnitudes of momenta in the two-body c.m. system[47]). Since this amplitude indeed possesses in the P plane all the poles (and no other) of $\hat{t}_l(P^2) \equiv \hat{t}_l(P, P, P)$, it may be written as

$$\hat{t}_l(p, P, p') = r_l(p, P)\hat{t}_l(P^2)r_l(p', P) + \tau_l(p, P, p'), \tag{A1}$$

where $r_l(p, P)$ and $\tau_l(p, P, p')$ have no poles in P. The function $r_l(p, P)$ is therefore defined up to an

arbitrary function which vanishes at the poles. The choice in Ref. 12 was based on considerations of analyticity. This led to taking simply

$$r_l^{(1)}(p,P)=\pm\int_0^\infty j_l(pr)V(r)f_l(r,-P)r\,dr, \qquad \text{(A2)}$$

where j_l is the spherical Bessel function and $f_l(r,-P)$ is the irregular solution of the Schrödinger equation behaving like $\exp i(Pr+l\pi/2)$ as $r\to\infty$. The potential[45]

$$V(r)=\int_\mu^\infty \sigma(\alpha)\frac{e^{-\alpha r}}{r}\,d\alpha, \quad \mu>0 \qquad \text{(A3)}$$

is assumed analytic in the right-hand plane $\mathrm{Re}\,r>0$ and well behaved at the origin and at infinity, i.e.,

$$V(r)=O(r^{-1-\epsilon}), \quad \epsilon<1, \quad \text{as } r\to 0$$
$$|V(r)|<\text{const}\, r^N e^{-\mu r}, \quad \mu>0, \ N \text{ real and finite, as } r\to\infty. \qquad \text{(A3')}$$

Equation (A2) provides the simplest expression which can be built with the available potential-scattering functions for the residue at the poles, but it does not have certain other desirable properties which may be wanted both for the decomposition (A1) and for the corresponding $r_l(p,P)$. In particular the separable part should conveniently satisfy by itself two-body unitarity, if it is expected to approximate the full off-shell amplitude. This is the case if $r_l(P,P)=1$ [then $\tau_l(P,P,P)=0$] and if $r_l(p,P)$ is real for real p and P. These properties are satisfied by the combination

$$r_l(p,P)=\frac{-i}{2PN_l(P^2)}\left[f_l(-P)\int_0^\infty j_l(pr)V(r)f_l(r,P)r\,dr+(-)^{l+1}f_l(P)\int_0^\infty j_l(pr)V(r)f_l(r,-P)r\,dr\right] \qquad \text{(A4)}$$

$$\equiv\frac{-P^l}{N_l(P^2)}\int_0^\infty j_l(pr)V(r)\varphi_l(r,P^2)r\,dr, \qquad \text{(A5)}$$

which differs from $r_l^{(1)}(p,P)$ by a term which vanishes at the poles in P. $f_l(P)$ is the Jost function and

$$N_l(P^2)=\frac{f_l(P)-f_l(-P)}{2iP}\equiv -P^l\int_0^\infty j_l(Pr)V(r)\varphi_l(r,P^2)r\,dr. \qquad \text{(A5')}$$

The function $\varphi_l(r,P^2)$ is the regular solution of the Schrödinger equation of energy P^2, behaving like $r^{l+1}/(2l+1)!!$ at the origin. As defined through (A5), $p^{-l}P^{-l}r_l(p,P)$ and thus $r_l^2(p,P)$ are obviously even functions both in p and P. Note that these functions are the same as those which were first introduced by Noyes[48] and Kowalski.[46]

The principal interest of an integral representation like (A5) is to express in a simple way the form factors in terms of well-known functions of potential theory.[49] By assuming the properties of these functions, we can therefore easily deduce those of the form factors, especially with regard to the off-shell momentum p.

In this connection, we note that the integral in (A5) *a priori* converges only for $|\mathrm{Im}p|-\mu+|\mathrm{Im}P|<0$ (remember that μ^{-1} is the range of the potential). For real values of P, this integral thus defines an analytic function in a strip of the p plane enclosing the real axis. Such a domain of analyticity can be extended both in p and P by rotating the contour of integration as done in Ref. 12. An additional extension is obtained by performing the analytic continuation separately for the two integrals in (A4) and in another representation of $r_l(p,P)$ which reads

$$r_l(p,P)=\frac{-P^l}{2N_l(P^2)}\left[\int_0^\infty h_l^{(1)}(pr)V(r)\varphi_l(r,P^2)r\,dr-\int_0^\infty h_l^{(2)}(pr)V(r)\varphi_l(r,P^2)r\,dr\right] \qquad \text{(A6)}$$

and which is equivalent to (A5) at least in the vicinity of $p=0$ and $P=0$ ($h^{(1)}$ and $h^{(2)}$ are the spherical Hankel functions of the first and second kind). One finds in this way that $r_l(p,P)$ is analytic, on the one hand outside the dashed domain in Fig. 8(a) and on the other hand outside the dashed domain in Fig. 8(b). This shows that $r_l(p,P)$ may be considered as analytic everywhere in the p plane except along four vertical cuts starting from[50] $p=\pm P\pm i\mu$ as shown in Fig. 9(a). [The related cuts of $r_l^2(p^2,P)$ in the p^2 plane are shown in Fig. 9(b) for real and positive P^2.]

Further branch points of $r_l(p,P)$, $p=\pm P\pm ni\mu$ (n integer) as well as the analyticity domain of the function $\tau_l(p,P,p')$ in (A1) or of the full amplitude $\hat{t}_l(p,P,p')$ can be determined in a similar way.[12] As concerns the latter, singularities are found at[50]

$$\pm p\pm p'=ni\mu, \qquad P=\pm p-ni\mu,$$
$$P=-ni\mu/2, \qquad P=\pm p'-ni\mu \qquad \text{(A7)}$$

(n integer ≥ 1). All have the same physical origin as the usual singularities $P=\pm ni\mu/2$ of the on-shell amplitude.[51] Note that for real p and p', $\hat{t}_l(p,P,p')$ is free from singularity in the upper half P plane. On the other hand, for the real and positive P^2, p^2, and p'^2 values involved in the three-body equations in the scattering region, all the branch points in the p^2 and p'^2 planes lie outside the parabolas $\mathcal{P}(\mu^2)$ defined by

$$p^2 \text{ or } p'^2=(x+i\mu)^2, \quad x \text{ real} \tag{A7'}$$

and shown in Fig. 10. These parabolas indeed bind a domain of analyticity for $\bar{t}_l(p^2,P,p'^2)=p^{-l}p'^{-l}\hat{t}_l(p,P,p')$. Clearly, the larger the μ, i.e., the shorter the range of the two-body forces, the larger the extension of this domain and the farther the singularities from the physical p^2 and p'^2 positive values.

The threshold and asymptotic behaviors in p of $r_l(p,P)$ and $\hat{t}_l(p,P,p')$ are also easily derived from the integral representation (A5) and from that (2.12) of Ref. 12 [$t_l(r,P,p')$ in the latter has the same relevant properties as $\varphi_l(r,P^2)$]. For both functions, the threshold behavior can be deduced by expanding the Bessel function at small p values in these representations, which gives $O(p^l)$. In a similar way, the asymptotic behavior is related to the sine transform of $V(r)\varphi_l(r,P^2)$ or $V(r)t_l(r,P,p')$. One gets $O(p^{-l-2})$ for $\epsilon>0$ in (A3'), $O(p^{-l})$ for $-2<\epsilon<0$, and so on, which shows that, as expected, the asymptotic behavior depends on the shape of the potential near $r=0$.

Lastly, let us remark that, instead of starting as in Ref. 12, from previously known results of potential theory, one can as well deduce all the above properties from a direct analysis of the Lippmann-Schwinger integral equation for $t_l(p,P,p')$. This has been done in Refs. 20 and 21. By the way, integral representations of $\hat{t}_l(p,P,p')$ in the off-shell variable p have been written down, the method used in Ref. 20 being more easily generalizable to relativistic equations like the Bethe-Salpeter ones.[52]

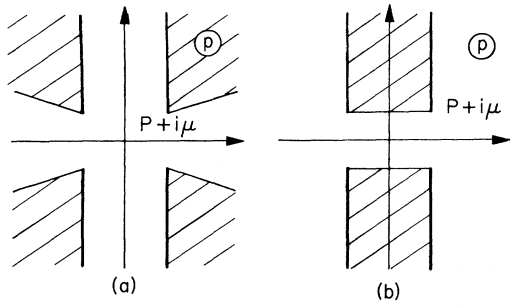

FIG. 8. Determination of the analyticity domain of the form factors $r_l(p,P)$ in the p plane: (a) as deduced from the representation (A4), (b) as deduced from the representation (A6).

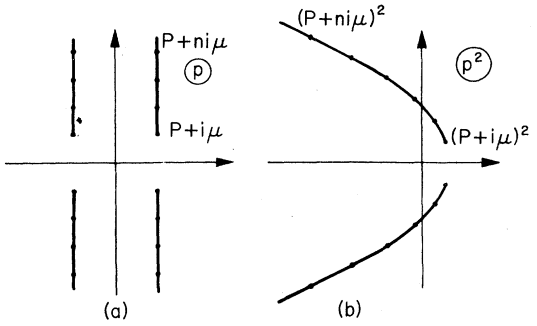

FIG. 9. The resulting cuts and branch points (a) of $r_l(p,P)$ in the p plane, (b) of $r_l^2(p,P)$ or $p^{-l}r_l(p,P)$ in the p^2 plane.

2. Comments on the Reliability of Some Simple Separable Approximations

Now we may try to take advantage of the above results to get information on some separable approximations of the form

$$t_l^S(p,P,p')=p^l p'^l \frac{\bar{g}_l(p^2)\bar{g}_l(p'^2)}{D_l(P^2)} \tag{A8}$$

which may be used in the three-body equations for representing the true $\hat{t}_l(p,P,p')$ amplitude associated with (A3). The threshold and asymptotic behaviors as well as two-body unitarity can be easily introduced in (A8). Indeed, two-body unitarity makes this representation almost determined once $g_l(p)=p^l\bar{g}_l(p^2)$ is known [see Eq. (2.11)]. Clearly, however, this single-variable function alone cannot accurately account for all the peculiarities of the three-variable amplitude

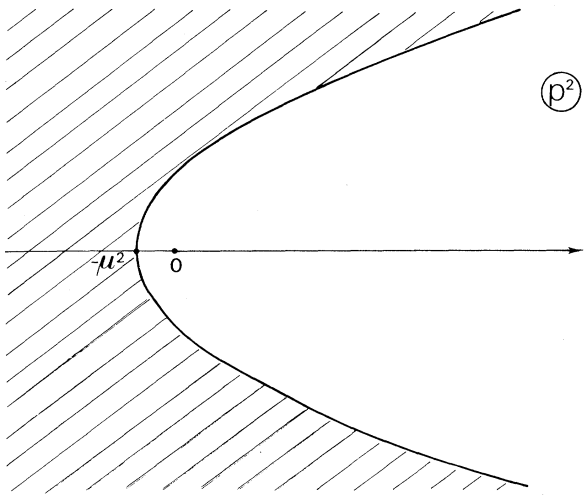

FIG. 10. The parabola $\mathcal{P}(\mu^2)$ defined in the p^2 (or p'^2) plane by Eq. (A.7') and outside of which lie the singularities of the off-energy-shell two-body amplitude involved in the three-body equations.

$\hat{t}_l(p,P,p')$. One can nevertheless require that the singularities and associated cuts of $t_l^S(p,P,p')$ stand for some average of those of $\hat{t}_l(p,P,p')$ in the three-body integral equations. This means in particular that

(i) in the P plane, $D_l(P^2)$ can only have singularities in the lower half part, which is trivially satisfied owing to Eq. (2.11);

(ii) in the p^2 plane, $g_l^2(p)$ can only have singularities outside the smallest analyticity parabola $\mathcal{P}(\mu^2)$, that is, $\mathcal{P}(4)$ for the $\pi\pi$ case.

This supplementary nontrivial condition, together with the fact that, as assumed in the present calculations, $D_l(\sigma)^{-1}$ has a well-defined resonance pole on its second sheet, is not yet sufficient to determine (A8) completely, unless some peculiar parametrizations are used. Further assumptions whose reliability is more doubtful must then be made:

(A) A first possibility is to assume, as many authors do, that $t_l^S(p,P,p')$, which indeed stands for some average in the three-body equations of the true $\hat{t}_l(p,P,p')$ amplitude, also reduces for $p^2 = p'^2 = P^2$ to the on-shell one $\hat{t}_l(P^2)$. Then $g_l(p) = [N_l(p^2)]^{1/2}$, while according to (2.11) and to (3.7) the related functions $D_l(\sigma)$ and $\delta_l(\sigma)$ are, respectively, the true on-shell $\hat{D}_l(\sigma)$ function of $\hat{t}_l(P^2) = N_l(P^2)/\hat{D}_l(P^2)$ and the experimental phase shift. But the above analyticity requirements associated with the rather reasonable interaction (A3) are then no longer necessarily satisfied, since theoretically $N_l(p^2)$ may have singularities at $p^2 = -\mu^2/4$, which lie inside $\mathcal{P}(\mu^2)$. [In practice, however, the requirement of analyticity can be fulfilled by choosing consequently the parametrization of $N_l(p^2)$.] Simultaneously, the residue at the resonance (second sheet) pole $\sigma_R = P_R^2$ becomes proportional to $[N_l(p^2)]^{1/2}[N_l(p'^2)]^{1/2}$ instead of

$$R_l(p,p') = \xi(P_R)\, r_l^{(1)}(p,P_R)\, N_l(P_R^2)\, r_l^{(1)}(p',P_R)\,, \tag{A9}$$

which follows from (A1) $[r_l^{(1)}(p,P_R) \equiv r_l(p,P_R)]$. This means that the off-shell dependence in the vicinity of the resonance pole cannot be the correct one associated with (A3): Indeed, the analytic properties of $N_l(p^2)$ and $r_l^{(1)}(p,P_R)$ are different, the latter alone being automatically compatible with the analyticity requirements.

(B) Contrarily, it is equally natural to assume the correct off-shell behavior near the resonance pole, that is, to take[53] [see Eq. (A9)]

$$g_l(p) = [\xi(P_R)]^{1/2}\, r_l^{(1)}(p,P_R)\,[N_l(P_R^2)]^{1/2}\,, \tag{A10}$$

which does not give again, when inserted in (A8), the true on-shell amplitude $\hat{t}_l(P^2)$ for $p^2 = p'^2 = P^2$. In other words, the procedure corresponds to just keeping[12] the separable part of (A1) with the off-shell dependence of the form factors at the pole. Indeed (A8) is only truly valid near this point, which moreover corresponds to the most conspicuous feature introduced in the present three-body model. In this case, the function $D_l(P^2)$ in (A8), which is related to $g_l^2(p)$ through Eq. (2.11), has only to equal the on-shell function $\hat{D}_l(P^2)$ at $P^2 = P_R^2$ where both indeed vanish. Therefore, the phase $\delta_l(\sigma)$ of $1/D_l$ [see Eq. (3.7)] appears above all as a convenient intermediate quantity and has no reason to equal the experimental phase shift except near the resonance energy [in fact, because P_R^2 is complex, the condition $D_l(P_R^2) = 0$ can be expressed in terms of conditions over $\delta_l(\sigma)$ and its first derivative at $\sigma_r = \mathrm{Re}P_R^2$].

To satisfy simultaneously the analyticity requirements and the basic assumptions retained in (A) *and* (B) would necessitate considering energy-dependent representations of the type

$$\tilde{t}_l(p,P,p') = \frac{\tilde{g}_l(p,P)\,\tilde{g}_l(p,P)}{\tilde{D}_l(P^2)} \tag{A11}$$

with

$$\tilde{g}_l(p,P_R) = [\xi(P_R)]^{1/2}\, r_l^{(1)}(p,P_R)\,[N_l(P_R^2)]^{1/2}$$

and

$$\tilde{g}_l^2(P,P) = N_l(P^2)\,,$$

that is, according to (2.11), $\tilde{D}_l(P^2) = \hat{D}_l(P^2)$, which means that the δ_l function entering a representation like (3.7) for $\tilde{D}_l(P^2)$ would be identified with the experimental phase shift. The choice $\tilde{g}_l(p,P) = [N_l(P^2)]^{1/2} r_l(p,P)$ associated with the separable part of (A1) satisfies these two constraints but, as is well known, leads in the three-body equations to difficulties due to the singularities of $N_l(P^2)$ [among others, the trace of the kernels in (3.14) would then not be real below the three-body threshold; see, for instance, Ref. 9]. This does not, nevertheless, preclude the possibility of finding other two-variable functions $\tilde{g}_l(p,P)$ which do not possess this defect. Assuming, for instance, the contributions of those singularities (A7) which depend on both the initial and the final variables being negligible – this is mainly true near the resonance pole – we can indeed build functions having only the two complex cuts of Fig. 9(b).

To conclude about the choice (A8), we can argue that the functions $g_l(p)$ and $D_l(P^2)$, which in the three-body equations best represent the effects of the true $\hat{t}_l(p,P,p')$ amplitude, can only satisfy each of the above assumptions (A) and (B) in a more or less approximate way according to the energy region. Therefore, in the calculations, we have retained some aspects of both possibilities.

First, we have kept an arbitrariness on the δ_l function as is found in (B), which allows us among other things to easily relate our results with preceding ones. On another side, we have retained the reality properties of the $g_l(p)$, which are easily warranted in (A) but would have required the consideration of at least two separable terms with (B) (see footnote 53).

---

*This work has been the object of a communication at the Birmingham Conference, 1969 [J.-Y. Pasquier and R. Pasquier in *Three-Body Problem in Nuclear and Particle Physics,* edited by J. S. C. McKee and P. M. Rolph (North-Holland, Amsterdam, 1970)].

†Laboratoires associés au Centre National de la Recherche Scientifique.

‡The revised version was sent by the authors after an extensive delay in the editorial processing.

[1]L. D. Faddeev, Zh. Eksp. Teor. Fiz. 39, 1459 (1960) [Sov. Phys. JETP 12, 1014 (1961)].

[2]E. E. Salpeter and H. A. Bethe, Phys. Rev. 84, 1282 (1951).

[3]D. Stojanov and A. N. Tavkhelidze, Phys. Letters 13, 76 (1964); V. P. Shelest and D. Stojanov, *ibid.* 13, 253 (1964).

[4]R. Blankenbecler and R. Sugar, in *Proceedings of the Twelfth International Conference on High-Energy Physics, Dubna, 1964,* edited by Ya. A. Smorodinskii *et al.* (Atomizdat., Moscow, 1966); R. Blankenbecler and R. Sugar, Phys. Rev. 142, 1051 (1966).

[5]V. A. Alessandrini and R. L. Omnès, Phys. Rev. 139, B167 (1965).

[6]D. Freedman, C. Lovelace, and J. M. Namyslowski, Nuovo Cimento 43, 258 (1966).

[7]A. Ahmadzadeh and J. A. Tjon, Phys. Rev. 147, 1111 (1966); J. M. Namyslowski, *ibid.* 160, 1522 (1967); R. Aaron, R. D Amado, and J. F. Young, *ibid.* 174, 2022 (1968); N. Mishima, S. Oryu, and Y. Takahashi, Progr. Theoret. Phys. (Kyoto) 39, 1569 (1968). Another somewhat equivalent procedure based on a more detailed knowledge of the analytic structure of the Bethe-Salpeter amplitude is reported in Ref. 20.

[8]C. Lovelace, Phys. Rev. 135, B1225 (1964).

[9]J. L. Basdevant, Phys. Rev. 138, B892 (1965); J. L. Basdevant and R. Kreps, Phys. Rev. 141, 1398 (1966); 141, 1404 (1966); 141, 1409 (1966); J. L. Basdevant, thesis, Université de Strasbourg, France (unpublished).

[10]J. L. Basdevant and R. L. Omnès, Phys. Rev. Letters 17, 775 (1966); in *Three-Particle Scattering in Quantum Mechanics,* edited by J. Gillespie and J. Nuttal (Benjamin, New York, 1968), and communication at the Fourteenth International Conference on High-Energy Physics, Vienna, 1968 (unpublished).

[11]J. F. L. Hopkinson and R. G. Roberts, Nuovo Cimento 59, 181 (1969).

[12]J. Y. Guennégués-Pasquier, Nuovo Cimento 42, 549 (1966).

[13]It is worth mentioning that the results obtained with G parity $G = +1$ in the $K\bar{K}\pi$ case equally apply to the $KK\pi$ (or $\bar{K}\bar{K}\pi$) systems.

[14]The study of this system was the object of a preliminary report, G. Mennessier, J.-Y. Pasquier, and R. Pasquier, Orsay Report No. TH 68/26, 1968 (unpublished).

[15]M. Jacob and G. C. Wick, Ann. Phys. (N.Y.) 7, 404 (1959); L. F. Cook and B. W. Lee, Phys. Rev. 127, 283 (1962); D. Branson, P. V. Landshoff, and J. C. Taylor, *ibid.* 132, 902 (1963); J. Werle, Phys. Letters 4, 127 (1963); Nucl. Phys. 44, 579 (1963).

[16]S. M. Berman and M. Jacob, Phys. Rev. 139, B1023 (1965).

[17]It is worth mentioning that in the $K\bar{K}\pi$ and $K\pi\pi$ cases, the same result remains valid even with an arbitrary number of two-body resonances in the $K\bar{K}$ and $\pi\pi$ subsystems, provided that there is only one resonance in the $K\pi$ (or $\bar{K}\pi$) subsystem.

[18]P. Baillon *et al.*, Nuovo Cimento 50, 393 (1967); Ch. d'Andlau *et al.*, Nucl. Phys. B5, 693 (1968).

[19]B. French, in *Proceedings of the Fourteenth International Conference on High-Energy Physics, Vienna, 1968,* edited by J. Prentki and J. Steinberger (CERN, Geneva, 1968).

[20]J. Y. Pasquier, part of a thesis to be submitted at the Université de Paris-Sud (unpublished).

[21]D. D. Brayshaw, Phys. Rev. 167, 1505 (1968).

[22]R. Omnès, Nuovo Cimento 8, 1244 (1958).

[23]M. G. Olsson, Phys. Rev. 162, 1338 (1967).

[24]R. Pasquier and J.-Y. Pasquier, Phys. Rev. 170, 1294 (1968); 177, 2482 (1969), and numerical results about the three-pion resonances, Ref. 25.

[25]R. Pasquier and J.-Y. Pasquier (unpublished).

[26]I. J. R. Aitchison, Nuovo Cimento 51A, 249 (1967).

[27]Note that this remark makes full sense only if we believe – although this leads elsewhere to other difficulties – in assumption (A) of part 2 of the Appendix. Indeed, to our knowledge, a correspondence between the sign of the scattering length and the nature of the two-body forces is usually considered only for the on-shell amplitude and this on the basis of qualitative results observed with some particular choices of potentials. It seems more difficult to obtain something similar for the behavior of the off-energy-shell amplitude $\hat{t}_l(p, P(\sigma), p')$ near $p = 0$. Such a behavior indeed depends on P and p'.

[28]See, for instance, I. J. R. Aitchison, Cambridge University report, 1966 (unpublished).

[29]J. H. Hetherington and L. H. Schick, Phys. Rev. 134, B935 (1965); 139, B1164 (1965); 141, 1315 (1966); I. M. Barbour and R. L. Schult, *ibid.* 155, 1712 (1967).

[30]Similar results are also observed in the other J^P channels, but with often many more difficulties because of the coupling of the equations (e.g., $J^P = 1^+$ or 2^-), or because of the more complicated angular functions involved in the kernel (e.g., $J^P = 2^+$).

[31]Note some discrepancies between the results of Table II(a) and those given in Refs. 9 and 10.

[32]Almost all the low mass resonances put for completeness in Tables II(a) and III(a) are indeed not observed experimentally. Comparatively, the absence of so many unexpected resonant states appears at first sight as one nice property of Tables II(b) and III(b).

[33]Of course, owing to conservation laws, each $g^G(J^P)$

channel is differently affected by the contribution of other two-body components, couplings with inelastic channels, or omitted three-body left-hand cuts. This might be simulated by choosing differently (according to the J) the values of the parameters, namely c in Eq. (3.9). The procedure would have then resulted in a much better agreement with experiment in each J, in particular the characteristics of the ω can be much better reproduced than indicated in Table III(b). By keeping for all J the same c value as done in the present work, one gets nevertheless a simpler and more consistent picture in all quantum states of the $\rho\pi$ (K^*K), if not of the full $\pi\pi\pi$ ($K\bar{K}\pi$), system.

[34]R. Vanderhagen *et al.*, Phys. Letters 24, 493 (1967).

[35]This possibility is examined in Ref. 20 with methods somewhat analogous to those of Ref. 36.

[36]R. E. Kreps and P. Nath, Phys. Rev. 152, 1475 (1966).

[37]J. L. Basdevant, D. Bessis, and J. Zinn-Justin, Phys. Letters 27, B230 (1968).

[38]One does not reasonably expect to find the φ meson under the present approximations, since its three-pion decay mode is largely dominated by the $K\bar{K}$ one. Note, as regards the ω, that attempts for finding it in terms of $\pi\rho$ interaction have been first made by G. F. Chew, Phys. Rev. Letters 4, 142 (1960), and A. Ahmadzadeh, LRL Report No. UCRL 11749, 1964 (unpublished).

[39]Taking into account the influence of the mean value of the two-body amplitude on the three-body results, one can however expect such a property to be only true for types I and III, as discussed in Ref. 25. Indeed, it is shown in this reference that a different but in some sense more natural effect can be observed with type II, namely that the narrower the two-body resonance, the broader the three-body one (the higher its mass).

[40]Note that this result from decay analysis may indeed not be contradictory with ours on the related three-body resonance, since the former concerns the complete solution of the equations, while the latter concerns only the Fredholm determinant.

[41]R. F. Peierls, Phys. Rev. Letters 6, 641 (1961); 12, 50 (1964); and D. D. Brayshaw and R. F. Peierls, Phys. Rev. 177, 2539 (1969). See also the work of C. Schmid, Ref. 42.

[42]A. H. Rosenfeld, LRL Report No. UCRL 16462, 1965 (unpublished); C. Schmid, Phys. Rev. 154, 1363 (1967).

[43]N. Barash-Schmidt, A. Barbaro-Galtieri, Leroy R. Price, A. H. Rosenfeld, P. Söding, C. G. Wohl, M. Roos, and G. Conforto, Rev. Mod. Phys. 41, 109 (1969).

[44]This is part of a separate work by two of us (J.-Y. P. and R. P.) which provides the natural extension of Ref. 12 and is inserted here for completeness (see also Ref. 20). The two authors thank Professor K. Chadan for discussions about this work.

[45]Of course, there is no well-established reason for believing that the true off-energy-shell meson-meson amplitude can be built up on the basis of such a local potential. Perhaps it is easier to admit, owing to some analogy with other problems, that this potential represents the longest-range part of the interaction – note, however, that the lowest exchanged state is already composed with two pions – while the shortest one requires the introduction of "nonlocal" terms, often approximated by separable forms. Then, as the following analysis indeed suggests, one can argue that the first part gives rise to the most restrictive constraints on the analyticity domains and therefore is the most relevant for our discussion.

[46]K. L. Kowalski, Phys. Rev. Letters 15, 798 (1965); 15, 908 (1965).

[47]P^2 is denoted s in Ref. 12. In relativistic kinematics, P is related to the squared energy-invariant σ through an equation like (2.12′) (In this Appendix, the use of P, instead of σ, as the on-shell variable of $\hat{t}_l$, allows one to handle expressions like those currently encountered in the nonrelativistic case.) Similar relations hold for the off-shell quantities p and p' and the corresponding off-shell squared invariant energies.

[48]H. P. Noyes, Phys. Rev. Letters 15, 538 (1965).

[49]See, for example, R. G. Newton, J. Math. Phys. 1, 319 (1960).

[50]In relativistic approaches, similar formulas are found but μ has to be considered as the mass of the particle (or of the system of particles), whose exchange gives rise to the two-body forces.

[51]T. Regge, Nuovo Cimento 9, 295 (1958); A. Martin, *ibid.* 14, 403 (1959); 15, 99 (1959).

[52]R. Pasquier and J.-Y. Pasquier (unpublished).

[53]Of course, an additional term associated with $\sigma_R^* = P_R^{*2}$ has also to be included in order to warrant the reality properties of $g_l^2(p)$.